Heart Rate Measurement using a 60 GHz Pulsed Coherent Radar Sensor

Linn Gromert & Melina Alnasser

2022

Master's Thesis in Biomedical Engineering

Supervisors: Erik Månsson, Martin Stridh

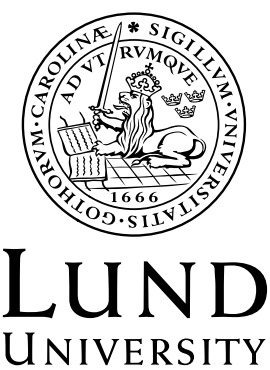

Faculty of Engineering LTH Department of Biomedical Engineering

Thesis for the degree of Master of Science in Biomedical Engineering.

Department of Biomedical Engineering
Lund University
P.O. Box 118, SE-221 00 LUND, SWEDEN

Abstract

Heart rate is today measured in various ways, but they all include contact with the skin. Measuring heart rate contactless would be a more efficient method in healthcare and would also benefit people suffering from skin problems. It has been proven that it is possible to use radar to measure heart rate. The aim of this thesis is to investigate how to extract the heart rate with a 60 GHz pulsed coherent radar sensor.

The heart rate was measured by aiming the radar sensor at the chest. This study included use of different radar configurations, distances to the participants and tilting angles of the radar sensor. An electrocardiogram was used as a reference signal during the collection of these measurements. During the preprocessing phase, two different approaches of removing the movement caused by respiration were tested: A bandpass filter and principal component analysis. Furthermore, two different methods for heart rate estimation were tested: One method based on detecting minima of the signal and the other method consisted of a recurrent neural network. During the evaluation, the heart rate provided by the sensor signal was compared to the heart rate of the ECG signal.

The conclusion of this work was that the best measurement setup was achieved when measuring with a tilted sensor with a beam aimed at the participant's chest. The sensor was placed in front of the patient at a distance of 0.4 meters. To remove the respiration, applying an adaptive bandpass filter to the unwrapped phase turned out to be the best solution. The minima detector got the most accurate result when comparing to the reference signal. The majority of heart rates estimated based on these steps had a small difference when compared to the reference signal.

Acknowledgments

This master thesis work has been done at Acconeer AB in Malmö during spring term 2022 as a final work for our degree in Biomedical Engineering. We would like to thank the system team at Acconeer for their help and support. A special thanks to our supervisor Erik Månsson who has been welcoming and helping since day one. It has been a pleasure to be a part of the company. We would also like to thank our supervisor at LTH, Martin Stridh, for the guidance during the whole project.

Linn Gromert & Melina Alnasser

List of Acronyms and Abbreviations

ANN Artificial Neural Network

CNN Convolutional Neural Network

CZT Chirp Z-Transform

DFT Discrete Fourier Transform

ECG Electrocardiogram

EM Electromagnetic

E-Plane Elevation-Plane

FFT Fast Fourier Transform

FZP Fresnel Zone Plate Lens

HBL Hyperbolic Lens

H-Plane Horizontal-Plane

HPBW Half Power Beam Width

LSTM Long Short-Term Memory

PCA Principal Component Analysis

PCR Pulsed Coherent Radar

Radar Radio Detection And Ranging

ReLU Rectified Linear Unit

RNN Recurrent Neural Network

SNR Signal-to-Noise Ratio

UWB Ultra-Wideband

Contents

Chapter 1
Introduction

Today, plenty of devices that measure heart rate exist on the market, for example pulse oximeters or watches. However, the most common device used at hospitals is the electrocardiogram, ECG, which requires electrodes attached to the patient's body. It gives more visual information about the signal which is used to discover heart diseases more easily. However, it would be beneficial to be able to measure heart rate in a contactless way as it gives more mobility. This means that the patient would not be bothered about wires and electrodes being placed on them. This type of method for measuring heart rate is essential for patients who suffer from skin problems such as burns or allergies to the sensor pads. Since no device has to be cleaned after usage it will result in a faster examination, which decreases the work load at the hospitals. There are also environmental aspects that has to be considered. By using less disposable material, for example the sensor pads that are used to attach the electrodes to the patients body, it will favor the environment.

Measuring movement on the body surface of the chest using a radar sensor has been a useful technique when measuring vital signs in a contactless way. In the article *Contactless Real-Time Heartbeat Detection via 24 GHz Continuous-Wave Doppler Radar Using Artificial Neural Networks* it is stated that it is possible to detect heart beats by using Continuous-Wave doppler radar together with an artificial neural network [16].

One major difficulty when using radar to measure heart rate is the respiration, which causes a much larger movement of the body than the heart. In the previous mentioned article [16] no preprocessing of the data is made before sending it in to the ANN, however this approach may not be possible using other kinds of radar sensors. Depending on the type of radar sensor, the signal will have to be preprocessed in different ways to obtain the information of interest.

1.1 Our Project

This master thesis covers different methods to measure and extract heart rate, also called pulse, with a 60 GHz pulsed coherent radar sensor from Acconeer AB. By

combining our biological and technical knowledge, our goal is to find an accurate way of extracting the heart rate. To do this, the following questions are investigated:

- Which configuration and setup should be used when measuring the small chest motions caused by the heart beats?
- What processing method is the most convenient to use to remove noise from the signal?
- How can the heart rate be estimated from the processed data?

The different measurement setups will all include the radar beam being aimed at the upper part of the chest. Also, this project was limited to only examine heart rate at rest and the test persons had to sit as still as possible during the measurements. This was done in order to avoid possible noise sources, which scaled down the problem. However, the movement of the body due to breathing still existed and was a big challenge during this thesis.

1.2 Related Work

In the article *Principal Component Analysis for Heart Rate Measurement using UWB Radar* [11], Principal Component Analysis (PCA) was used to find the vital signs when measuring with an Ultra-Wideband (UWB) impulse radar. The measurements were made on a person breathing normally and seated 0.9 meters from the radar sensor. The UWB radar measured the small movements of the thorax caused by heart beats. These movements are smaller than the movements caused by respiration, which means that the respiration will act as noise in the measured signal.

The purpose of using PCA is to increase the signal-to-noise ratio which will result in that the vital signs, both respiration and heart rate, may be easier extracted. The input to the PCA was a 2D matrix containing the raw data. The article mentions that the first principal component is the one that contains the most important information about the vital signs and also contains the least amount of noise. The Chirp Z-Transform, CZT, is used on the first principal component, which gave a higher frequency resolution of the signal compared to using FFT. Three different signal processing approaches are compared in the article; Complex Signal Decomposition, Fast Fourier Transform and PCA. The conclusion was that PCA is the most optimal method to use when extracting vital signs from measurements of an UWB radar.

In the article mentioned in the introduction, *Contactless Real-Time Heartbeat Detection via 24 GHz Continuous-Wave Doppler Radar Using Artificial Neural Networks* [16], data was gathered from 21 participants; 14 males and 7 females. The participants were told to sit on a chair at a 0.75 m distance from the sensor and breath normally in a relaxed state. The radar beam was focused on the torso area and the beam widths of

the antenna at -3dB were 25° and 44°. ECG was used as a reference signal and was converted to a binary on/off signal. The binary reference signal and the radar signal was decimated to the same sampling rate of 100 Hz. This rate was chosen to ensure fast computation without a loss of information. Each recording session consisted of 200 seconds of normal breathing. The input to the Artificial Neural Network, ANN, was however a 200-sample long vector. The first 100 samples were the in-phase signal and the following 100 samples were the quadrature signal. A subpart of 100 samples corresponds to 1 second of recording. The network had an hyperbolic tangent activation function and was trained by using Levenberg-Marquardt optimization and a MSE loss function. The output neuron used a sigmoid function. The output of the network was ANN detection probabilities. These were passed through a moving average filter and then a peak detector was used to get the detected heartbeats.

It was shown that a basic ANN outperformed more complex networks. The simple ANN, a network with a single hidden layer containing 10 units, did not have the capacity to overfit and therefore had a more general model. However, this can be related to that the database for training was limited. Using an ANN was a significant improvement in the computational complexity compared to the FFT-based approaches.

1.3 Outline of the Report

The report is divided into the following parts:

- **Chapter 2: Background**

  The essential theory considering radar sensors, signal processing and ECG are described.

- **Chapter 3: Method**

  This chapter describes the different setups when collecting the data, preprocessing of both ECG and the sensor data and how to estimate the heart rate.

- **Chapter 4: Results**

  Tables and graphs presents the result of the different measuring setups and preprocessing techniques. The estimated heart rate based on the sensor signal is presented together with the heart rate given by the reference signal.

- **Chapter 5: Discussion and Conclusion**

  The presented results are discussed and the optimal measuring technique is stated. Possible sources of error will be brought up.

Chapter 2
Background

2.1 Signal Processing Basics

2.1.1 Complex Notation

A complex number can be represented in different forms. The easiest form is the Cartesian form, also called rectangular form. A complex number c is in this form expressed as

$$c = a + jb, \tag{2.1}$$

where a is the imaginary part and b the real part. The magnitude M of the complex number c is defined as

$$M = |c| = \sqrt{a^2 + b^2} \tag{2.2}$$

and describes how far, regardless of the direction, the variable differs from zero. The phase angle ø can be calculated according to the following equation [15]:

$$\text{ø} = tan^{-1}(\frac{b}{a}) \text{ radians} . \tag{2.3}$$

The result is only defined between $-\frac{\pi}{2}$ and $\frac{\pi}{2}$. To obtain a result in the correct quadrant, defined between -π and π, arctan2 has to be used [22].

Phase wrapping is an artifact when calculating the phase of the signal. It arises when the value of the phase is restricted to a fixed period and only one value is used in the computations [6]. This results in jumps of 2π. To get a continuous phase signal, a process called phase unwrapping can be done. If the difference between two samples is larger than π then the current sample and the samples to the right are shifted with -2π. If the difference is negative, then the samples are shifted with 2π [9].

2.1.2 Variance and Signal-to-Noise Ratio

The variance, σ^2, describes the effect of the signal's fluctuations from the mean and can be expressed as

$$\sigma^2 = \frac{1}{N}\sum_{n=1}^{N}[x(n) - \overline{x}]^2, \tag{2.4}$$

where $x(n)$ denotes any sequence value and $\overline{x}$ is the sequence average. The square root of the variance is called *standard deviation*.

The signal-to-noise ratio can be used to quantify the quality of a noise-contaminated signal. This is done by using the following [15]:

$$SNR = \frac{\text{Signal power}}{\text{Noise power}}. \tag{2.5}$$

2.1.3 Filters

A filter is characterised by that it passes signal components of some desired frequencies while it stops signal components of other undesired frequencies [20]. Several different types of filters can be used to remove unwanted frequencies in the signal, for example lowpass filters, highpass filters and bandpass filters. A bandpass filter, as the name implies, passes one frequency band and attenuates frequencies above and below that band. A highpass filter only passes high frequencies and attenuates low frequencies, and vice versa for lowpass filters.

The filter order describes the highest exponent in either the numerator or denominator of the z-domain transfer function of a digital filter. Generally it can be said that the larger filter order, the better the frequency selection performance is, but the computational workload also increases.

A recursive filter, also called Infinite Impulse Response (IIR) filter, have in many cases more computational advantages in both speed and storage requirements compared to an equivalent non-recursive filter [7, 27]. One example of a recursive filter is *Bidirectional* recursive filtering. In this case both forward and backward filtering is applied. During forward filtering the filter moves from left to right. The filter moves in the opposite way during backward filtering. Bidirectional recursive filtering produces a zero phase, meaning that the impulse response is symmetrical around sample zero. The only downside with the use of this technique is that the execution time and program complexity increases with a factor of two [27].

Filters can be based on the mathematical function Bessel. This function produces the most linear phase response of all IIR filters. Filter design based on Bessel functions have most constant group delay. If a filter's phase is not constant, in other words is a nonlinear-phase filter, then group delay distortion occurs because signals at different frequencies take different time to pass through the filter [15].

2.2 The Fourier Transform

The Fourier Transform is a method to transform a function, described as a time series, from the time domain to the frequency domain. The continuous time Fourier Transform of x(t) is defined as

$$X(f) = \int_{-\infty}^{\infty} x(t)e^{-j2\pi ft}\,dt, \tag{2.6}$$

where $X(f)$ is the frequency domain signal that consists of a real- and an imaginary part, where f is the continuous frequency and t corresponds to the time.

When having a discrete time signal, the Fourier Transform is instead called the Discrete Time Fourier Transform (DTFT) and is defined as

$$X(f) = \sum_{n=-\infty}^{\infty} x(n)e^{-j2\pi fn}\,dt, \tag{2.7}$$

where n correspond to each data point.

The Discrete Fourier Transform (DFT) is defined as

$$\bar{X}(k) = \frac{1}{N}\sum_{n=0}^{N-1} x(n)e^{\frac{-j2\pi nk}{N}}\,dt, \tag{2.8}$$

where N is the amount of samples in the sequence and k is the discrete frequency [13]. The DFT is called real DFT if only one time domain signal exists. The data can also be complex instead of real, which is the case in this thesis. A complex DFT's time domain signal consists of two signals, one with the real- and one corresponding to the imaginary-part [27].

The Fast Fourier Transform (FFT) is an algorithm used to compute the DFT more efficiently than when using other methods. The FFT consists of less complex additions and multiplications compared to the DFT, which is why the method is computationally faster [8].

The frequency f is defined as [21]:

$$f = 1/T, \tag{2.9}$$

where T is the period of time measured in seconds.

2.3 The Heart Activity

The heart is composed of two halves, where each half consists of an atrium and a ventricle. Systole and diastole are the two work phases of the heart. During systole the ventricle muscles start contracting and the blood leaves the ventricles. During diastole the ventricles get filled up with blood from the atrium [19].

The inflation and deflation of the lungs causes the chest surface to move from 4 to 12 mm. The frequency range of this motion is between 0.1-0.7 Hz. The heart also causes chest motions, but they are small compared to the respiratory motion of the chest. The chest motion caused by the heart ranges from 0.2 to 0.5 mm and is in the frequency range of 0.75-3 Hz , which corresponds to 45-180 beats per minute. Further, these motions overlap spectrally which makes it difficult to separate these signals [11, 25]. The heart rate is approximately 70 beats per minute during rest and increases when active. In an active condition, the heart rate can be over 100 beats per minute [19].

2.3.1 The Electrocardiogram

The Electrocardiogram, also called ECG, is a device that measures electrical activity of the heart by attaching electrodes to the body surface. The amount of electrodes depends on the purpose of the measurement. When the heart rhythm is measured, fewer electrodes can be used compared to when information about the waveform morphology is needed.

The nomenclature used to define the different parts of the ECG is composed of five letters; P, Q, R, S and T. The QRS complex defines the depolarisation of the ventricles of the heart [18]. The depolarization triggers muscular contraction. The ventricles start to contract during the R peak [14]. The QRS complex is shown in figure 2.1.

The ECG signal can consist of QRS complexes with different morphologies due to technical issues or physiological aspects. Sometimes the P or T waves have larger amplitude than the QRS complex, which result in that they sometimes get misinterpreted as being a part of the QRS complex. Baseline wander is an artifact that usually has a frequency of 0.5 Hz and is created by different kinds of body movements, for example respiratory activity. If the body movement is too large, the ECG signal will be completely distorted [28]. According to article [12], the ECG signal mostly consist of frequencies between 0.25 Hz to 35 Hz, which means that it is necessary to use a lowpass filter to remove high frequency noise from the ECG signal.

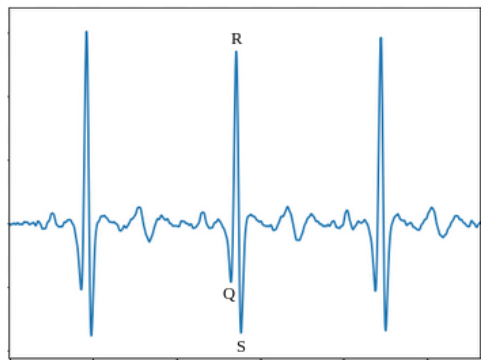

Figure 2.1: An ECG signal containing three heart beats where the QRS complex is defined. The signal is measured by using an Arduino microcontroller together with a Sparkfun AD8232 chip.

2.4 Radar

2.4.1 Radar Basics

Radar is a system that uses radio-frequency electromagnetic wavelets to detect objects in a specific region. Radars can have a frequency in the range of 3 MHz up to 300 GHz, however most radars operate in the range of 300 MHz to 35 GHz. A specific radar system does not operate over the entire range, instead it has a design band that decides the frequencies. In the early days of radar systems, radar usage was limited. Today, radar can be used for military and civilian tracking of aircraft and vehicles, collision avoidance and earth resources monitoring [24]. Many radars have an output signal that is complex instead of real-valued, also called coherent [23]. Radar systems can differ in many ways, however what they all have in common is that they consist of:

- Transmitter: Sends out the EM waves.
- Antenna: The connection between the transmitter/receiver and the medium (for example the air). There are two common antenna configurations called *bistatic* and *monostatic*. Bistatic refers to having two separate antennas for the transmitter and the receiver. The monostatic on the other hand means using a shared antenna for the transmitter and the receiver.
- Receiver: Receives the EM waves that have reflected on the object. The signal is amplified and converted to an intermediate frequency or a baseband signal. Finally it is analog-to-digital converted (ADC).
- Signal processor: Analyses and sorts the data and returns a measurement result [24].

The time between when the pulse was sent away and when it comes back to the antenna is measured, Δt, and together with the speed of the radio wave, c, it is possible to find out the distance to the object, R [5]. The speed of the radio wave corresponds to the speed of light, c. The formula for the distance to the object is defined as [23]:

$$R = \frac{c\Delta t}{2}. \tag{2.10}$$

Continuous and *pulsed* are two different classes of radar waveforms. Continuous means that the transmitter is continually sending out a signal without any interruptions. Pulsed instead means that a sequence of pulses is transmitted at a time, and between each sequence the radar is turned off for a set time. The waves usually have a time duration, or pulse width, of 0.1 to 10 μs, however sometimes it can be as short as just a few nanoseconds.

A radar system can be either *coherent* or *noncoherent*. A noncoherent radar system only detects the amplitude of the signal, which is used to find the location of an object. Coherent is the most common radar system and means that the system detects both the amplitude and the phase of the signal. It is therefore possible to determine changes in the phase, which gives information about the motion of the object [24].

2.4.2 Acconeer's Radar Sensor

Acconeer is a company that develops 60 GHz pulsed coherent radar sensors. A Pulsed Coherent Radar (PCR) sends out pulses with radio wavelets. The radar is bistatic; one of the antennas transmits the radio wave, which bounces back on the object and is received by the second antenna. The transmitter shuts down between the pulses, which results in a lower power consumption. The time between when the signal is transmitted and when the signal is received is measured to determine the distance to the object [5].

A transmitted signal with the frequency 60 GHz is in the millimeter range and is therefore a part of the class mmWave and is considered as a short wavelength. A benefit with using short wavelengths is that the detection of small movements will be possible, therefore the accuracy is high. Another advantage is that the size of the system components can be small [30].

The radar Acconeer produces is called *A111*. They are currently working on a prototype which aims to be the next generation sensor and is called *A121*. The A111 sensor has been used in different use cases. For example detecting if a parking space is occupied or not and measuring water level in manholes [2].

Configurations

Measurements with the radar sensor can be made using the *Acconeer Exploration Tool* that can be found on GitHub [3]. Here it is possible to adjust how the data should be

collected. Parameters that can be set here are *profile*, *HWAAS*, *sweeps per frame*, *frame rate*, *start point*, *number of points* and *step length*.

- Profile: Controls the duration and shape of the emitted pulses. In this project only two profiles will be used, profile A and B. Profile B has a longer pulse than profile A. Generally shorter pulses give higher distance resolution and the signal-to-noise ratio decreases.

- HWAAS (Hardware Accelerated Average Samples): Sets the amount of radar pulse averaging in the sensor. When increasing the HWAAS, the radar loop gain also increases but every sweep will take longer time which will limit the maximum update rate.

- Sweeps per frame: Every frame consists of a number of sweeps, which is controlled by this parameter. A sweep is a distance measurement range. Each sweep ranges from a start point and continues for a set sweep length. Each sweep contains one or several distance sampling points.

- Frame rate:
$$f_f = \frac{1}{T_f}, \tag{2.11}$$
where T_f is the time between two following frames.

- Start point: Sets the starting point for the sweep.

- Number of points: Number of points in each sweep.

- Step length: The distance between the points. If the step length is set to one, the distance between the points will be 2.5 mm [5, 17].

Service - Sparse IQ

In Acconeer Exploration Tool it is also possible to choose a service, which sets the output type. The selection of service should be based on what the use case is. Acconeer's prototype A121 uses a service called *sparse IQ*, which produces complex data points which are sparsely sampled. Every sweep gives a vector of complex data points. Since the data points are complex, it means that the phase and amplitude of the signal can be calculated [17].

An example of the real part of the data recorded with the service *sparse IQ* is shown in figure 2.2 below. The recording contains information of the different settings of the sensor, time stamps of each sample and the measured data. The blue/yellow area represents an object being in front of the sensor.

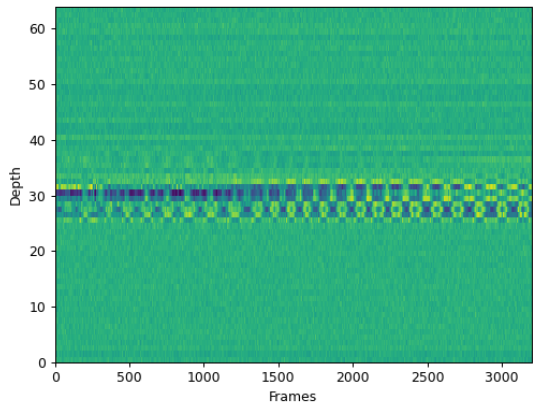

Figure 2.2: The graph describes on what depth the object is positioned. Each point in y-direction corresponds to approximately 2.5 mm.

Reflectivity

The radar sensor gets different amount of energy back to its antenna depending on the object. The factors that determines the energy is the reflectivity of the object (γ), the radar cross section of the object and the distance to the object.

Reflection appears when the radar signal propagates trough a new media with a different relative permittivity than the previous media. The relative permittivity is frequency based. Some materials together with their reflectivity are stated in table 2.1. These values are based on the radar frequency being 60 GHz and air being the other media [5].

Table 2.1: Different materials with their reflectivity based on that air is the previous media and the radar frequency being 60 GHz.

Material	γ
Mobile phone glass	0.02
Concrete	0.11
Wood	0.046
Textile	0.029
Metal	1
Human skin	0.22
Water	0.28

Lenses

Acconeer produces three different lenses in order to aim the radar pulses. The two lenses that will be used in this thesis are the *Hyperbolic lens* (HBL) and the *Fresnel Zone Plate* lens (FZP). These will be used together with Acconeer's lens holder *LH112*. This holder has two different positions to put the lens in, referred to as D1 and D2. The lenses are positioned at 3 mm respective 8.2 mm from the sensor when using D1 and D2, respectively. The difference between the half power beam width (HPBW) for the lenses is presented in the table below. The HPBW radiation pattern determines the angle between the half power (-3 dB) points of the main lobe of the radiation pattern.

Table 2.2: The half power beam width in the E- and H-Plane when using the HBL and FZP lens.

Lens	**HPBW E-plane (°)**	**HPBW H-plane (°)**
HBL	15	20
FZP	25	12

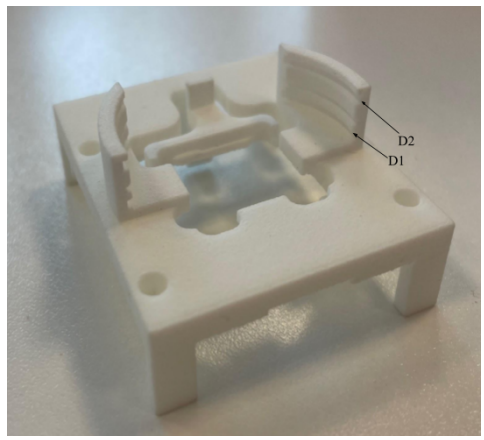

Figure 2.3: The LH112 lens holder and the two different positions for the lens; D1 and D2.

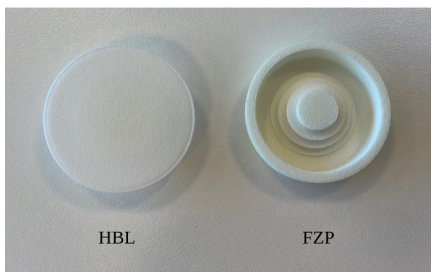

(a) The lenses side towards the sensor.

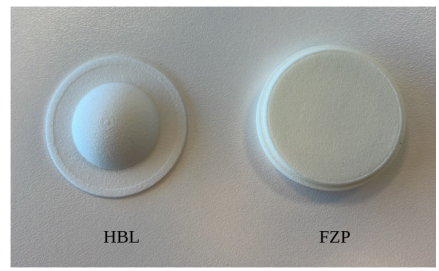

(b) The lenses side towards the measuring object.

Figure 2.4: The HBL and FZP lenses.

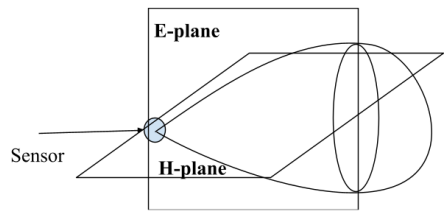

Figure 2.5: The elevation plane and the horizontal plane for the transmitted sensor signal.

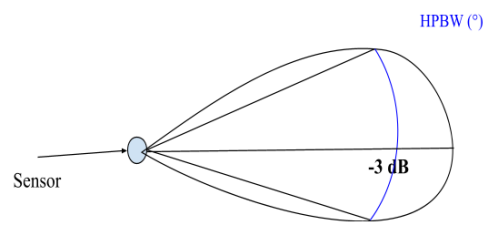

Figure 2.6: Visualisation of half power beam width.

Using a lens will also improve the range where the object will be visible. In the tables below the difference in range when not using a lens and using the Fresnel lens will be presented for two objects. These results are based on using profile A and a service called *envelope*. An object counts as visible if SNR is bigger than 10 dB [5].

Table 2.3: Ranges for two different objects when using profile A and the envelope service without using a lens.

Object	**0.5 m**	**1 m**	**2 m**	**5 m**
Head	Visible	Visible	Not visible	Not visible
Torso	Visible	Visible	Visible	Not visible

Table 2.4: Ranges for two different objects when using profile A, the envelope service and the Fresnel lens.

Object	0.5 m	1 m	2 m	5 m
Head	Visible	Visible	Visible	Not visible
Torso	Visible	Visible	Visible	Visible

2.5 Recurrent Neural Network

Recurrent Neural Network (RNN) is a family of neural networks that can handle varying lengths of the input and can be useful when modeling sequences in the form of time series. It also has an ability of memorizing information, which means that it takes into consideration how the current sample depends on the previous sample [29]. However, some of the RNNs have a tendency to cause a gradient problem, which means that the gradients gets very small. This results in that for each new input, the memory of the earliest samples of the network will be lost. It therefore means that these samples will no longer influence on the output of the network.

Long Short-Term Memory (LSTM) is a recurrent neural network that contains a specific amount of memory blocks. Each memory block contains memory cells and three multiplicative units; input-, output- and forget gates. The multiplicative units are nonlinear summation units and are in control of the activation of the cell. The LSTM network is similar to a standard RNN, however the memory blocks replace the summation units that exists in the hidden layer of the RNN network. The LSTM removes the gradient problem since the multiplicative gates allow the memory cells to keep the information during a longer time [10].

2.5.1 Activation Functions

The choice of activation function is important to obtain good performance when training a neural network. One common activation function is the non-linear function called *Rectified Linear Unit* (ReLU). This is an efficient function, since not all the neurons are activated at the same time. The ReLU activation function is defined as

$$f(x) = max(0, x). \tag{2.12}$$

Another common activation function is called *sigmoid* and is a non-linear function. Sigmoid is defined as the equation below;

$$\sigma(x) = \frac{1}{1 + e^{-x}}. \tag{2.13}$$

The gate activations vary between 0 and 1, where 0 means that the gate is closed and 1 correspond to that the gate is open. When having a binary classification problem, sigmoid is the most common activation function to use in the architecture.

Hyperbolic tangent function, also called tanh, is similar to sigmoid but the values vary between -1 and 1. It is defined as

$$f(x) = 2\textbf{sigmoid}(2x) - 1. \tag{2.14}$$

2.6 Principal Component Analysis

Principal Component Analysis (PCA) is a mathematical method to reduce the dimension in the data but still keep the variation in the dataset. The main purpose of using this method is to extract the most important information that exist in the data. PCA finds orthogonal variables called *principal components* that correspond to the variability of the data. This makes it possible to represent the data with less variables than the original data. The first principal component is said to be the one that represents the main part of the variation in the data and therefore contains the valuable information.

The PCA method is obtained by finding out the eigen-decomposition from either the correlation or covariance matrix. The eigen-decomposition of a matrix consists of eigenvectors and eigenvalues and they describe the structure of the matrix. The eigen-decomposition can be defined as

$$AU = \Lambda U, \tag{2.15}$$

where A is the correlation or covariance matrix, U contains all the eigenvectors and Λ is the diagonal matrix containing the eigenvalues.

The PCA is performed by first calculating the covariance of the data. The PCA method thereafter use the *Singular Value Decomposition* (SVD) method to find the eigenvectors and eigenvalues of the covariance matrix. By applying the SVD on a rectangular matrix, three matrices are composed which constitute the eigen-decomposition. The SVD is defined as

$$A = P\Delta Q^T, \tag{2.16a}$$

$$\Delta = \Lambda^{\frac{1}{2}}, \tag{2.16b}$$

where P corresponds to the eigenvectors of the matrix AA^T. Q corresponds to the eigenvectors of the matrix A^TA [1][11].

Chapter 3
Method

The objective of our work was to develop and evaluate different ways to measure and extract the heart rate with a 60 GHz pulsed coherent radar sensor. This chapter will cover the performed steps to accomplish this. The work was divided into the following parts (see an overview in figure 3.1):

- **Equipment and Data Processing** (see section 3.1)
- **Measurement Trials** (see section 3.2)
- **Collect Larger Datasets** (see section 3.3)
- **Heart Rate Estimation** (see section 3.4)
- **Noise Removal Improvement** (see section 3.5.1)

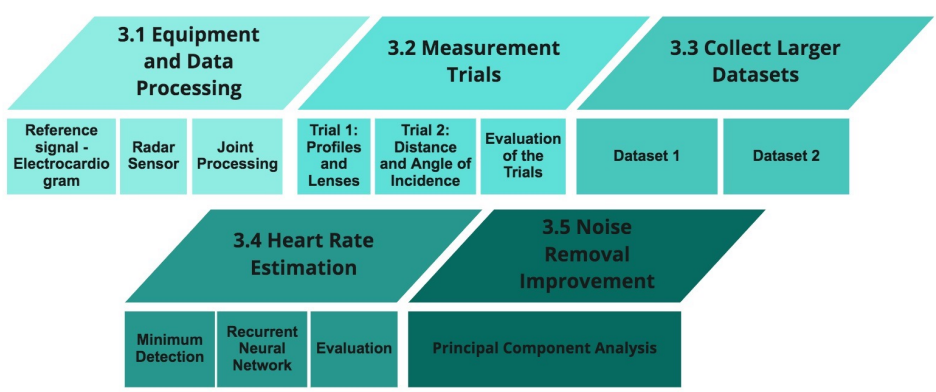

Figure 3.1: An overview of the method.

3.1 Equipment and Data Processing

In order to investigate the accuracy of measuring heart rate with a radar sensor, a reference signal corresponding to an electrocardiogram is used. The reference signal is measured at the same time as the sensor signal in order to evaluate the performance of the sensor signal. More information about how these measurements are performed are presented below. In figure 3.2 an overview of the separate preprocessing methods for the ECG and the sensor signal is shown. A more detailed explanation is described later on in this section. The preprocessing is done in Jupyter Notebook documents *.ipynb*, which are Python source coded files.

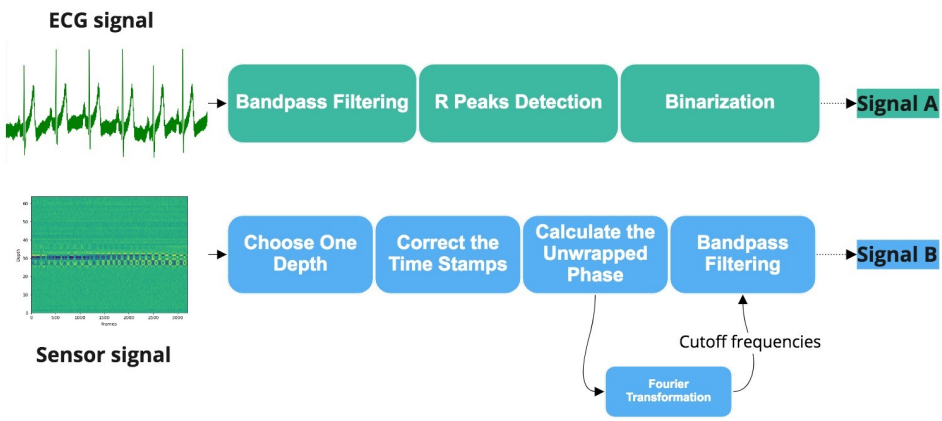

Figure 3.2: An overview of the processing of the ECG signal and the sensor signal.

3.1.1 Reference Signal - Electrocardiogram

Measurement Equipment

The electrical activity of the heart is measured using an Arduino microcontroller together with a Sparkfun AD8232 chip, which results in a real time monitored ECG signal. The sampling frequency for this signal is 2575 Hz. A 3-electrode system which consist of a red, blue and black electrode is used. These electrodes are placed according to the scheme that can be seen in figure 3.3a. The electrodes are attached to the participants skin with the gel on the biomedical sensor pads, see figure 3.3b.

(a) Instruction of where to attach the electrodes on the body.

(b) The electrodes and sensor pads used to measure ECG.

Figure 3.3: The electrodes of the ECG and their placement.

Preprocessing of ECG Signal

As earlier mentioned, ECG is used to get a measure of the correct heart rate. The ECG gives information about the electric activity of the heart dependent on time. In order to get a measure of the heart rate, each R peak of the electric activity, which would represent occurring heart beats, is counted. To make this possible, some preprocessing must first be performed.

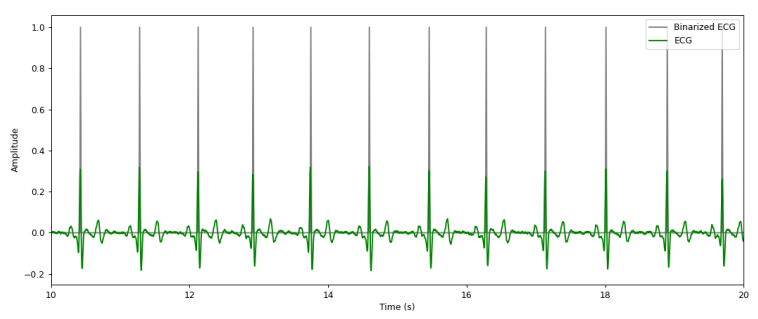

Figure 3.4: A filtered ECG signal is plotted in green. The binarized version of it is plotted in grey. The binarized signal is created by representing each R peak with a one and setting all the other samples to zero.

The ECG signal is preprocessed with a second order bandpass Bessel filter, which removes the unwanted frequencies corresponding to noise in the signal. This filter is selected as it has the most constant group delay and therefore has the least amount of group delay distortion. As it is a bandpass filter, a lower and higher cutoff frequency is decided. The starting values in this project are based on the ones presented in the article [12]. The lower limit is set to 0.25 Hz and the upper limit was given the value of 35 Hz. To improve the possibility of extracting the R peaks of the signal, different values of the lower limit is tested.

The next step is to extract the R peaks and thereafter binarize the signal. This is done by first dividing the ECG data into 20 subparts. The parts are equally divided if possible. If not, all parts except for the last one would be the same size and the last part would be a bit shorter than the rest. For each part the SciPy function *find_peaks* is applied. Both a minimum requirement of the height of the peaks and a minimum distance between the peaks are set in the function. The minimum height is adjusted for each part, however the minimum distance is the same for all the parts. For each subpart, the minimum height is set to 60% of the 3rd largest amplitude of the subpart. The minimum distance for the whole signal is decided by the following steps:

1. Calculate the median of the 50 largest amplitudes of the entire signal.
2. Use the function *find_peaks* with a height threshold of 70% of the median value.
3. Calculate the differences in time between adjacent peaks by using the NumPy function *diff*. The median value of these differences is thereafter computed.
4. The distance is set to 70% of the median value.

The *find_peaks* function returns the positions of the R peaks. To create a binarized signal, a new signal of the same size as the original signal is created where all values are set to zero. Then, for each returned position the value is set to one. However, some

peaks will be missing when using this method. Acconeer's internal labeling tool made it possible to handle this manually.

3.1.2 Radar Sensor

Measurement Equipment

The radar sensor is connected to a *Raspberry Pi 3 Model B* (2015) (see figure 3.5a), which is a single-board computer. A connector board called *XC112* is attached to the Raspberry Pi (see figure 3.5b). Acconeer's radar sensor prototype A121 is put on a radar sensor module named *XR112*. The sensor has a sampling rate of 30 Hz.

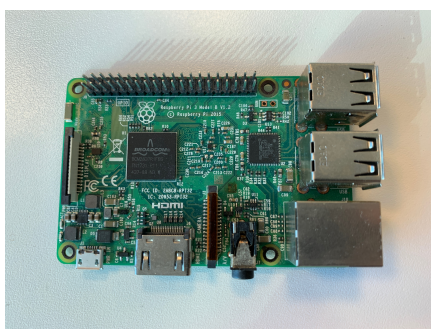

(a) Raspberry Pi 3 Model B.

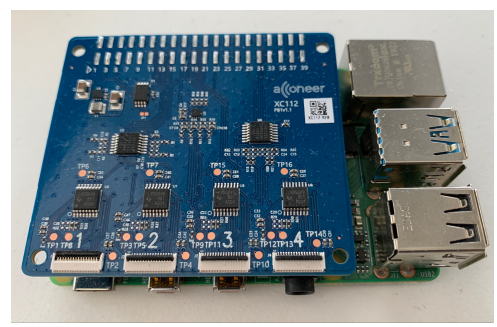

(b) The XC112 attached to the Raspberry Pi.

Figure 3.5: Sensor equipment.

Preprocessing of Radar Data

As mentioned in the background, the sensor data correspond to complex numbers and contains information for a range of depths, see figure 2.2. In order to use the collected data for heart rate estimation, some preprocessing has to be done:

1. The variance is calculated for each depth in the sensor signal. The one with the highest variance is chosen.

2. In some of the recordings, the time stamps of the sensor data is not entirely correct, this was solved using the NumPy polyfit function.

3. Since the phase of the signal is wrapped, unwrapping has to be performed. This is solved by using NumPy's unwrap function.

4. The discrete Fourier transform is applied to the unwrapped phase of the signal and the discrete Fourier transform frequencies are determined by using the functions *fft* and *fftfreq*.

5. The frequency with the maximum amplitude, f_M, in the range 0.8 to 1.9 Hz is determined. These frequencies correspond to 48 to 114 beats per minutes. The pulse can be both lower and higher values, however these frequencies are chosen as only the pulse at rest is investigated in this thesis.

6. A second order bandpass Bessel filter is designed by having the phase as input. The filter's cutoff frequencies are based on the frequency with the maximum amplitude f_M. However, since many signals contain low frequency noise, the cutoff frequencies are set to:

   (a) The lower cutoff frequency = $f_M - 0.2$.

   (b) The higher cutoff frequency = $f_M + 0.5$.

7. A forward backward filter is then applied to the output of the bandpass filter. This filter is chosen as it gives a zero phase.

3.1.3 Joint Processing

Since the recording of the ECG and the radar sensor does not start and end at the exact same time, the arrays have to be adjusted in order to be compared. An overview of the joint processing of the binarized ECG signal (signal A) and the sensor signal (signal B) can be seen in figure 3.6.

Figure 3.6: An overview of the joint processing.

1. The first step is to make the length of the sensor signal 10 times longer. A method based on the *interp* function is used. A parameter called q is used to regulate if the data is upsampled or downsampled and to which extent. To obtain upsampling a value smaller than 1 is chosen. If the goal is to downsample, a value larger than 1 should be used. In this case, q is set to 0.1.

   The reason for this is to make the time stamps of the ECG and sensor signal comparable, as the ECG signal is sampled with a higher sampling frequency.

2. Afterwards, the starting and ending points for the ECG and sensor signal are set. The signal with the latest starting point determine the starting point for

the new signals and the signal with the earliest ending point determine the end point for the signals.

The signals are thereafter downsampled in order to reduce the data size. This is done in the following steps;

1. The binarized ECG signal is first downsampled. To not lose important information, the signal is downsampled with a factor 5. The downsampling is done in a way that still retain the same amount of samples that are set to one, corresponding to heart beats.

2. The length of the sensor signal is adjusted to have the same length as the downsampled ECG signal. This is done by setting the parameter q in the *interp* function to the quota of the length of the sensor signal and the length of the ECG signal.

The last processing step is to remove 50 samples in the beginning and the end of the signals. This is done in order to prevent possible outliers. In total 100 samples are removed for both the ECG signal and the radar signal.

3.2 Measurement Trials

To investigate the impact of the measurement setup, recordings are performed using different profiles, lenses, distances to the test persons and with two different angles of the lens holder. These tests are divided into two trials and performed on 2-4 participants. Later in the work, larger data collections will be carried out with the setups that achieved the best results from these tests.

A Python script was written to be able to record the sensor data through Acconeer Exploration Tool. The configuration of the measurements are decided in the script. The script of the ECG recording used in this project was already written by Acconeer. To start the ECG and radar measurements at the approximately same time, a Bash script is used.

3.2.1 Trial 1: Profiles and Lenses

First of all, measurements with different profiles and lenses are investigated. As mentioned in section 2.4.2, the choice of profile decides the duration and shape of the pulses. Profile B has a longer pulse than profile A. The two lenses used in this part of the thesis, FZP and HBL, are described in section 2.4.2.

The measurements are done both when the test persons are holding their breath and when breathing normally. The movement of the chest due to respiration has been mentioned as a problem in previous related work. Measuring heart rate without breathing makes it possible to see how much the respiration motion affects the signal.

The measurements are made on people sitting on a chair approximately 0.7-0.9 meters in front of the sensor. The sensor is aimed at the chest of the person, which is regulated by changing the height of the table which the sensor is attached to. While recording, it is important that the person remain as still as possible, since both the sensor and the ECG device are sensitive to movements. In figure 3.7a and 3.7b, the measurement setup and the angle of the lens holder can be seen.

(a) An overview of the measurement setup, where the use of the radar sensor and the ECG can be seen.

(b) The lens holder horizontally attached to the table.

Figure 3.7: The measurement setup when testing different profiles and lenses.

The chosen values of the configuration parameters can be seen in table 3.1. A starting point of 100 means that the first measuring point will be at $100 \times 2.5mm = 250$ mm from the sensor. A step length of 8 correspond to $8 \times 2.5mm = 20$ mm and is the distance between each measuring point. Since the number of points is equal to 64, the distance to the last measuring point will be $64 \times 2.5mm + 250mm = 1530$ mm. This results in a measuring range of 0.25 to 1.53 m from the radar sensor.

Table 3.1: The chosen measurement configurations.

Profile	A & B
HWAAS	16
Sweeps per frame	1
Frame rate (Hz)	30
Start point	100
Number of points	64
Step length	8

Holding Breath

To reduce as many difficulties as possible, the test persons are holding their breath while measuring. This makes it possible to investigate how the signal behaves and how easy it is to actually extract the heart beats of the signal. To explore how the choice of profile affects the signal, both profile A and B are used while measuring. First of all, measurements are made on two people. The best profile is later on used during measurements on four people, of which two women and two men. All the measurements are approximately 20 seconds long and the FZP lens is used in the D1 position of the LH112 lens holder.

Normal Breathing

In this part of the investigation, measurements are made with the purpose of finding a good configuration when breathing normally. Profile A and B are used when measuring on two people. FZP and HBL are tested together with each profile and person. The lenses are put in the D1 position of the lens holder LH112. Measurements are also done without using a lens. In total 12 measurements are performed. See the different test combinations in table 3.2.

Table 3.2: The different tests using profile A or B combined with different lenses. These tests are performed on two persons.

Test	Profile	Lens
1	A	-
2	B	-
3	A	FZP
4	B	FZP
5	A	HBL
6	B	HBL

3.2.2 Trial 2: Distance and Angle of Incidence

In one of the articles mentioned in section 1.2 the radar has been positioned straight in front of the participants chest on a distance of 0.75 and 0.9 meters, which was approximately the set up used in the beginning of this thesis. However, with the hope of improving the results, new ways of measuring are now explored. All the new measurements are performed at a distance of 0.4 meters in front of the person and the lens holder of the sensor is tilted 18.5 degrees (see figure 3.8a). The angle is calculated using the values from figure 3.8b. The new measurement setup can be seen in figure 3.9.

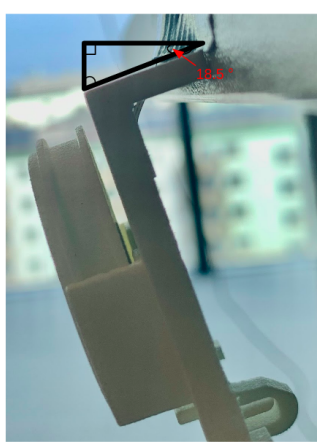

(a) The lens holder is tilted with an angle of 18 degrees.

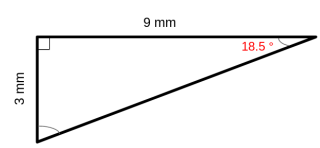

(b) A triangle describing the angle and distances of the tilted sensor.

Figure 3.8: The tilted lens holder.

Figure 3.9: The new measurement setup.

The FZP lens is used for these measurements together with profile A. Since the distance to the test person is shorter, the start point has to be decreased to 70 (see table 3.3). This means that the object must be placed in the range of 0.175 - 1.455 m from the sensor. However, the rest of the parameters are the same as in section 3.2.2. The measurements are performed on two people, one measurement when holding breath and one when breathing normally.

By calculating the unwrapped phase of the measured signals and thereafter applying the same bandpass filter as in section 3.1.2, it is visually possible to see if a pattern between the sensor signal and the ECG signal exist. To test this setup further, another 10 recordings of 60 seconds are made on each person. By increasing the amount of measurements it is possible to see if the received results are a coincidence or not.

Table 3.3: The chosen measurement configurations.

Profile	A
HWAAS	16
Sweeps per frame	1
Frame rate (Hz)	30
Start point	70
Number of points	64
Step length	8

3.2.3 Evaluation of the Trials

To evaluate the measurements, the heart rate given from the sensor signal is compared with the heart rate of the reference signal. The heart rate of the sensor signal is decided by manually counting the amount of minima in a plot of the signal phase. This is compared to the amount of R peaks in the ECG signal. The percentage of the amount of minima in the sensor signal with respect to the amount of heartbeats in the reference signal is calculated. The optimal case is that the sensor detects the same amount of heartbeats as the reference signal, in other words the percentage would be equal to 100. If the value is above 100 the sensor detects more heart beats than actually exists and vice versa.

3.3 Collect Larger Datasets

To continue the investigation on which setup that gives the most accurate result, two larger sets of data are collected during respiration. Both of these datasets are collected using profile A and the FZP lens in the D1 position. The difference between these datasets is explained more detailed below.

3.3.1 Dataset 1

The first dataset is measured at a distance of 0.7-0.9 meters from the participant. The measurements are made on ten people; three women and seven men. Two measurements are performed on each person, where each measurement was approximately two minutes long. To obtain a normal resting heart rate, the participant is left seated for at least 30 seconds before the measurement starts. The configurations used for these measurements are the same as in table 3.1.

3.3.2 Dataset 2

A second data collection is made at a distance of 0.4 meters and with the sensor tilted 18.5°, just like in figure 3.8a. The participants are five women and five men. Two measurements are done on each participant, where each measurement is 1 minute. Just as before, each participant is breathing normally and is supposed to sit as still as possible. The configurations that are set for these recordings are the same as presented in table 3.3.

3.4 Heart Rate Estimation

Two different ways of estimating the heart rate based on the filtered unwrapped phase of the sensor signal are tested. The first method, minimum detection, is based on the NumPy function called *find_peaks* and the second method correspond to a Recurrent Neural Network. The purpose of both of these methods is to determine the amount of heart beats in the signal and convert it to a measure of heart rate, which is compared to the heart rate given from the corresponding ECG data. These methods differ regarding how a segment of samples is classified as being a heart beat or not.

3.4.1 Minimum Detection

This method is based on counting the number of local minima in the filtered unwrapped phase signal. The function *find_peaks* is used together with a minimum distance requirement. Before using this function, the signal has to be inverted. This is done to obtain the minima from the function instead of the peaks. The requirement of the minimum time distance is based on the highest acceptable heart rate for this method, a frequency of 1.9 Hz (see step 5 in section 3.1.2). The minimum time distance, d_{min}, is decided using equation 2.9 in section 2.2.

$$d_{min} = \frac{1}{f} = \frac{1}{1.9} = 0.526s \tag{3.1}$$

Based on this calculation, the minimum time distance for the function is set to d_{min} = 0.5 s. All of the minima that are found with this method are counted as heart beats.

3.4.2 Recurrent Neural Network

The second method used to estimate the heart rate is a recurrent neural network. This method is divided into three parts; preprocessing, training and validation and test.

Preprocessing

The whole dataset of 20 measurements of sensor data and the corresponding 20 measurements of the ECG data are used. Before dividing the 20 measurements into the

training or validation set, the order of the measurements are randomized. This is done due to the fact that the two measurements that belong to the same person are adjacent. The new randomized order is the same for the ECG measurements as for the sensor measurements. Thereafter, the first 80 % of the samples are put into the training set and the remaining 20 % are put into the validation set.

All of the recordings are divided into windows which each contain 40 samples. Each window of the ECG measurements is set to either 0 or 1. This is used as the ground truth for the windows of the sensor measurements. If a window of the ECG measurements contain a 1, then the ground truth value is set to 1. Therefore a one would represent that a heart beat is present in the window.

Training and Validation

The architecture of the recurrent neural network that is used can be seen in figure 3.10. The input to the neural network is a matrix of the size 40x1 and the output value is either a 0 or a 1. The training is divided into 10 epochs with a batch size of 8. The first dense layer consist of 200 units and the second consist of 1 unit. The model use the optimizer *adam* and the loss function *binary crossentropy*.

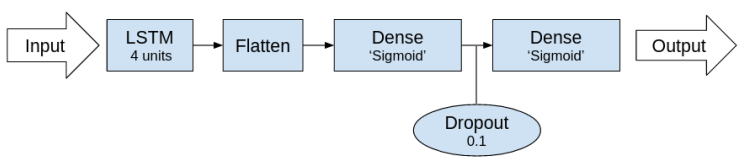

Figure 3.10: The RNN architechture.

Test

The measurements that are used for training and validation are also used for testing. One measurement is tested at a time. Predictions are made on the test data, which are used to evaluate the model. The amount of ones in the prediction are counted and used to get a measure of the heart rate.

3.4.3 Evaluation

Both of these methods are tested against the ECG signal in the same way.

1. The first step is to count the number of heart beats of the first 10 seconds of the signals. To get a measure of the heart rate, the number of heart beats are multiplied with the factor to get the corresponding heart beats per minute. The factor in this case is $\frac{60}{10} = 6$.

2. The second and third evaluation points are after 20 respectively 30 seconds. The same approach as in step one is applied here.

3. After 30 seconds, a sliding window is used. The window size is 30 seconds and the step length is 5 seconds. This is used until the end of the signal. For each window, the number of heart beats are multiplied with a factor 2 to get a measure of the pulse.

The heart rates are plotted as a function of the time in order to compare the pulse given from the reference signal with the pulse estimated from the sensor signal.

3.5 Noise Removal Improvement

The respiration creates a large movement on the body, which according to the articles mentioned in section 1.2 makes it difficult to extract the heart rate. Earlier in this method a bandpass filter was applied to remove the respiration from the phase signal. However, to examine whether it is possible to remove the respiration in better way, the Principal Component Analysis, similar to the one used in article [11], is used on both dataset 1 and 2 described in section 3.3.

3.5.1 Principal Component Analysis

As mentioned earlier in the report, a recording contain a 2D matrix of complex data corresponding to frames and depths. To find one of the depths where the object is located, the variance of each depth is calculated. Matrix X correspond to the depth with maximal variance and the surrounding 10 depths, which are sent in to the PCA algorithm.

The data is sent in to the NumPy Linalg function *svd* (Singular Value Decomposition) which returns two 2D matrices, U and V, and one singular value array, S. The reconstruction, R, of the signal is then calculated by using the following equation:

$$R = X(\bar{V}V), \tag{3.2}$$

where $\bar{V}$ is the complex conjugate of V. To reconstruct the signal using n principal components, the R matrix is calculated by choosing the first n columns of $\bar{V}$ and the first n rows of V.

For each depth, the unwrapped phase is calculated and sent into the PCA algorithm. The Fast Fourier Transform is thereafter calculated for the depth of the output containing the largest variance. This is done to extract the different frequencies of the signal.

Reconstructions containing three different number of principal components, $n = 1, 5$ or 9, are made for each dataset. The purpose is to analyze the FFT of each reconstruction and in that way find out if it is possible to remove the respiration from the original data to extract a signal showing the heart rate.

Chapter 4
Results

4.1 Data Processing

In this section, the result of processing the ECG and the sensor signal is presented. As will be shown below, processing of the signals was needed in order to estimate and compare the heart rates of the ECG and the sensor signal.

4.1.1 Electrocardiogram

Filtered ECG Signal

As earlier described, the aim was to calculate the reference heart rate by counting the number of R peaks in the ECG signal. In figure 4.1a the original ECG signal that is measured with the Sparkfun chip is shown. The signal contains some noise which makes it difficult to use a threshold to extract the R peaks of the ECG. A Bessel bandpass filter with the cutoff frequencies from [12] resulted in the signal in figure 4.1b. However, by increasing the lower limit, the R peaks got even more clear (see figure 4.1c). Because of this result, the lower limit of 5 Hz was thereafter used.

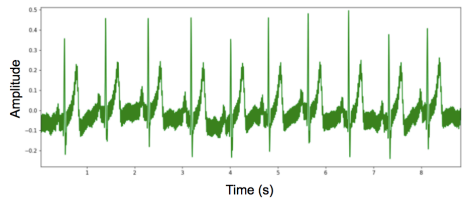

(a) Original ECG signal.

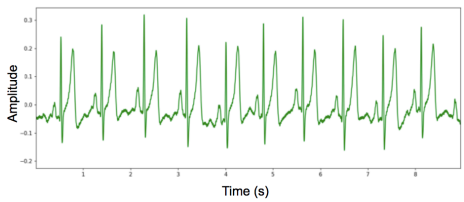

(b) Lower limit of 0.25 Hz.

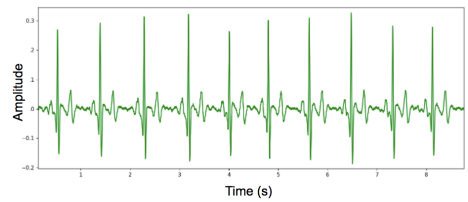

(c) Lower limit of 5 Hz.

Figure 4.1: The effect of bandpass filtering the ECG signal.

Binarization of the ECG Signal

With the aim of extracting the number of R peaks from the ECG signal, binarization was performed. The result of the binarization when using the function *find_peaks* with a height threshold as explained in section *Preprocessing of ECG Signal* (see 3.1.1) is shown in figure 4.2a. As can be seen, some peaks were not extracted by using this method and were therefore manually handled by using Acconeer's internal tool. The result of this can be seen in figure 4.2b.

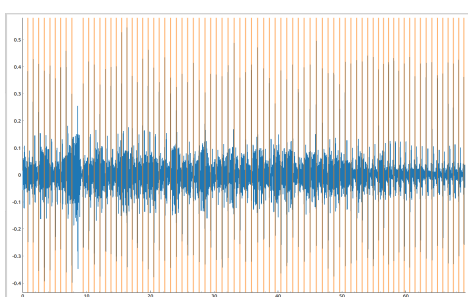

(a) The result of the binarization with the method explained in section 3.1.1.

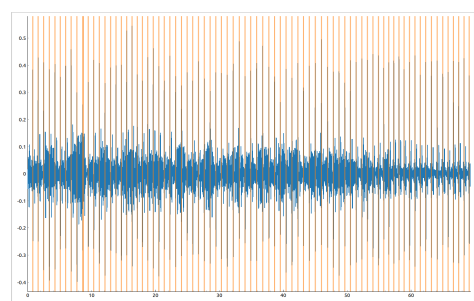

(b) The result after manually handling the binarization with Acconeer's internal tool.

Figure 4.2: The binarization of the ECG signal. The blue signal is the filtered ECG signal and the orange lines correspond to the binarization of the signal.

4.1.2 Radar Sensor

Time Stamps

The graph in figure 4.3a shows the time stamps of each sample for one recording. However, since the time stamps are supposed to be a linear graph, the polynomial fitting function corrected the error of each time stamp, see figure 4.3b. Now, each time stamp is connected to only one sample.

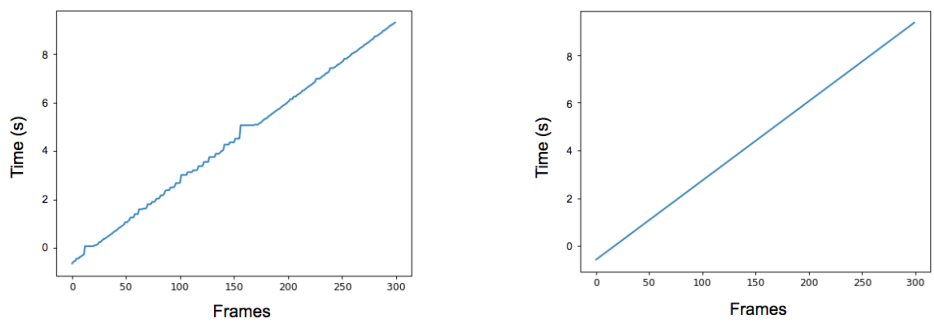

(a) The original time stamps.

(b) The time stamps after using the polynomial fitting function.

Figure 4.3: The result of using the polynomial fitting function in NumPy.

Unwrapping

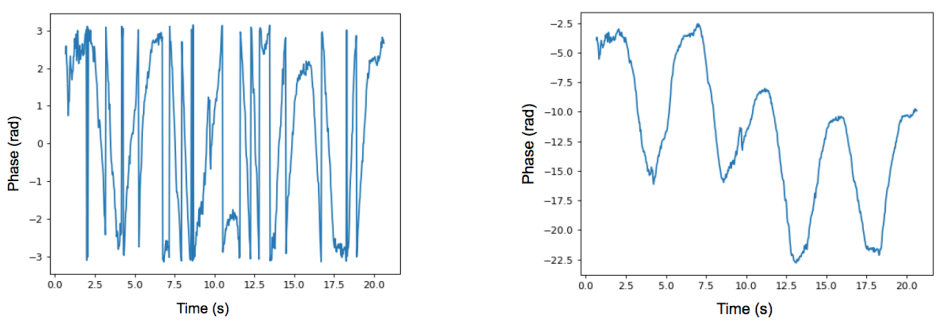

(a) The original phase signal.

(b) The unwrapped phase signal.

Figure 4.4: The result of using the NumPy function *unwrap*.

The phase of the signal is wrapped, which is shown by quick changes in the phase (see figure 4.4a). In figure 4.4b, the effect of using the NumPy function *unwrap* to solve these issues is shown. Unwrapping the phase results in a clear curve corresponding to the actual movements of the body.

4.1.3 Joint Processing

The ECG and radar sensor signal were adjusted to only consist of the time stamps where they both are recorded. Besides this, 50 samples from the beginning and the end of these signals were removed to prevent possible outliers. The result of this joint processing is shown below.

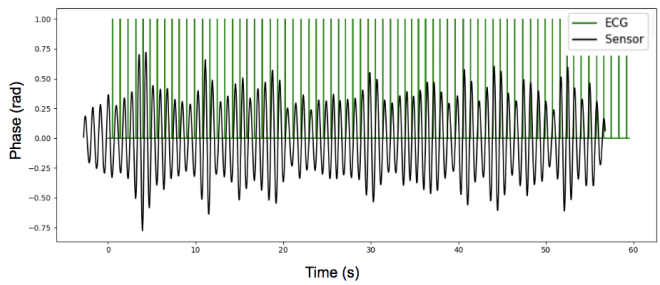

(a) The binarized ECG signal and the sensor signal before the joint processing.

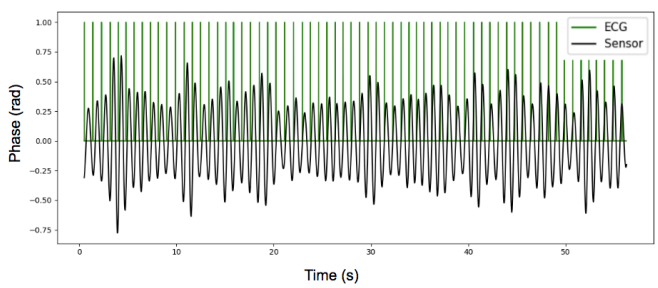

(b) The result of the joint processing. The signals now start and end at the same time.

Figure 4.5: The result of the joint processing for the binary ECG signal and the sensor signal.

4.2 Measurement Trials

In this section the results of using different lenses, profiles, distances to the sensor and the angle of the lens holder is presented. This was done both when the participants held their breath and when breathing normally.

To clarify the effect of holding the breath, the unwrapped phase for two measurements is plotted in figure 4.6. One example of the unwrapped phase of a signal where a person is holding their breath, is shown in figure 4.6a. As there is no respiratory activity, only small movements of the body have been recorded, such as the pulse. Figure 4.6b instead shows when the same person is breathing normally. The respiration causes larger body movements which result in a phase with larger amplitude.

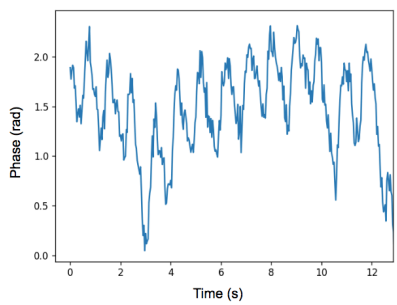

(a) This measurement is performed when a participant is holding the breath. The unwrapped phase of the signal is plotted.

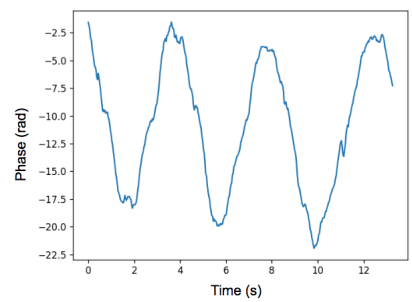

(b) The unwrapped phase of a measurement performed when a participant is breathing normally.

Figure 4.6: The unwrapped phases when holding the breath and breathing normally. Both measurements were made with profile A, lens FZP and on a distance of approximately 0.7 meters.

4.2.1 Trial 1: Profiles and Lenses

In this part the results of using different lenses combined with either profile A or B are presented. The goal was to investigate how the choice of profile and lens affect the resulting signal.

Holding Breath

Firstly, measurements where the participants held their breath were performed. For these tests, the FZP lens was used. The first test used both profile A and B when measuring on two people. The unwrapped and filtered phase of each measurement can be seen in figure 4.7. In figure 4.7a, 4.7b and 4.7d there seems to be an agreement in periodicity between the sensor and the ECG signal. Each minimum of the sensor signal occurs at approximately the same time as the R peak of the ECG. However, the sensor curve in figure 4.7c is not in sync with the ECG signal.

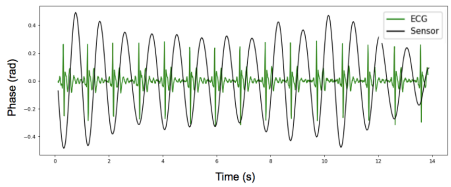

(a) Measurement 1: Person 1, where profile A was used.

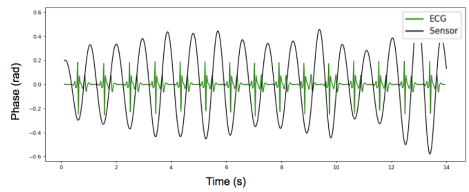

(b) Measurement 2: Person 1 when using profile B.

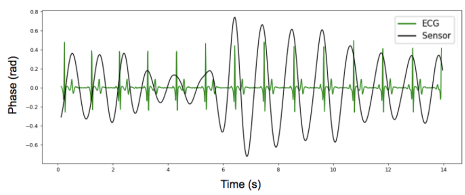

(c) Measurement 3: Person 2, where profile A was used.

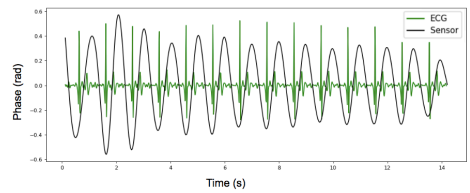

(d) Measurement 4: Person 2 when using profile B.

Figure 4.7: Measurement using profile A and B where the test persons hold their breath.

The number of minima were calculated in each of the measurements above and compared to the amount of heart beats in the ECG. The quota of these values is presented in the diagram in figure 4.8, where the optimal value is 100%. Measurement 1 and 3 used profile A and measurement 2 and 4 used profile B. When using profile B, the profile giving the longer pulse, good results were achieved. This is also the case for measurement 1, however not for measurement 3. Based on this, slightly better results were achieved when using profile B. Although, it is worth noting that both profiles gave good results.

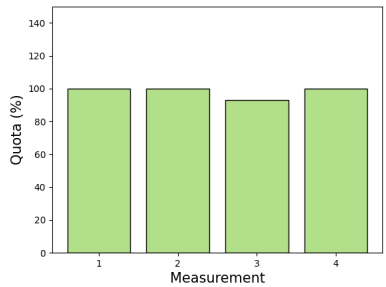

Figure 4.8: The quota between the number of minima of the sensor signal and the amount of heart beats of the ECG signal.

Due to this result, another test with more participants was made where profile B was used. The graphs below show the results when four people, two women and two men, hold their breath during the measurements.

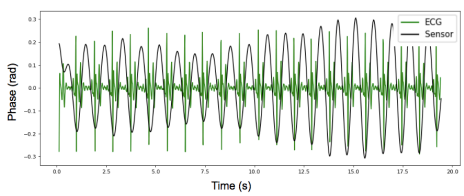

(a) Person 1.

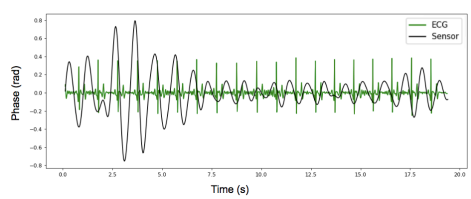

(b) Person 2.

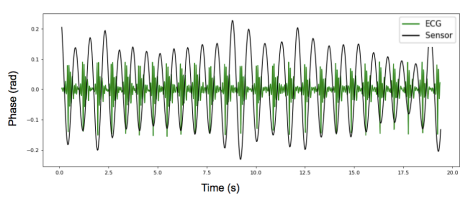

(c) Person 3.

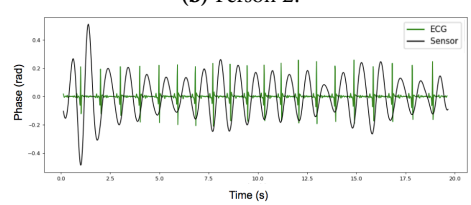

(d) Person 4.

Figure 4.9: Results of using profile B on four different persons holding their breath.

It is visually possible to see an agreement in the patterns between the peaks of the ECG and the minima of the sensor signal for three out of four persons. For these persons it is easily seen that the heart rate given from the sensor signal is the same or slightly differs from the reference signal. However, the pattern for the last person is not as clear.

Normal Breathing

Measurements were also performed when the participants were breathing normally. Here, both the profile and lens were varied. The measurement configurations that were tested are presented in section 3.2.1. These measurements were made on two people and the results for each person is presented in figure 4.10.

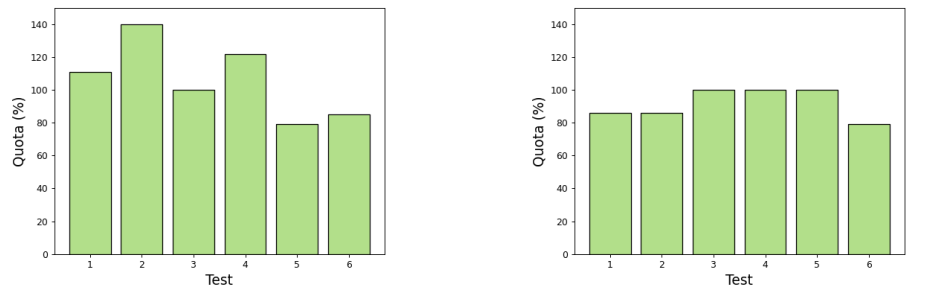

(a) The results for person 1.

(b) The results for person 2.

Figure 4.10: Quotas between the number of minima in the sensor signal and the number of R peaks in the ECG signal.

As can be seen in figure 4.10, test 3 gives the best result for both persons. This means that profile A together with the FZP lens gives the best result based on these tests. It can also be seen that for almost all measurements where the FZP lens is used (measurement 1, 3 and 5) the results are better than when using the HBL lens (measurement 2, 4 and 6).

4.2.2 Trial 2: Distance and Angle of Incidence

The results of measuring with a decreased distance, 0.4 meters from the participant, with a tilted lens holder are presented below. For all the measurements, the FZP lens and profile A were used. In figure 4.11 and 4.12, measurements on two people can be seen. Each figure contains one measurement when holding the breath and one when breathing normally. Here it is possible to see that the results are good, since the number of minima in the sensor signal compared to the number of peaks in the ECG signal is almost the same in all of the measurements.

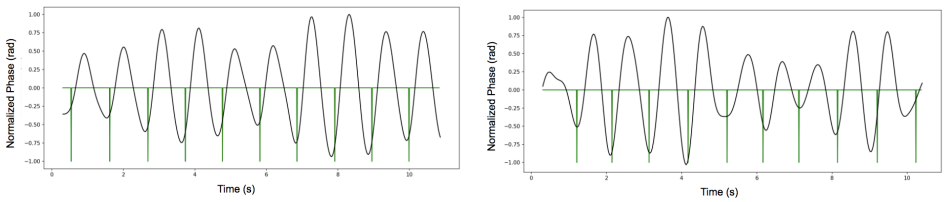

(a) Holding the breath. **(b)** Breathing normally.

Figure 4.11: Results for person 1.

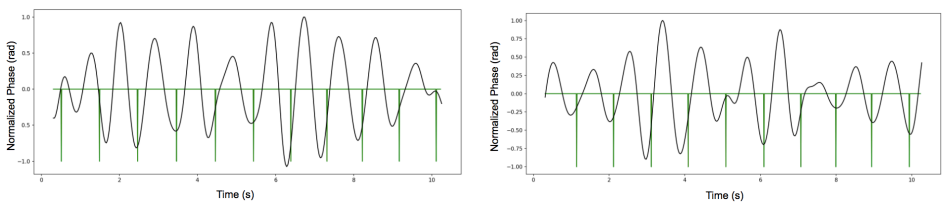

(a) Holding the breath. **(b)** Breathing normally.

Figure 4.12: Results for person 2.

To look deeper into this measurement technique, more measurements were performed on the same two persons. The results when doing 10 measurements on each person when breathing normally, is presented in 4.13.

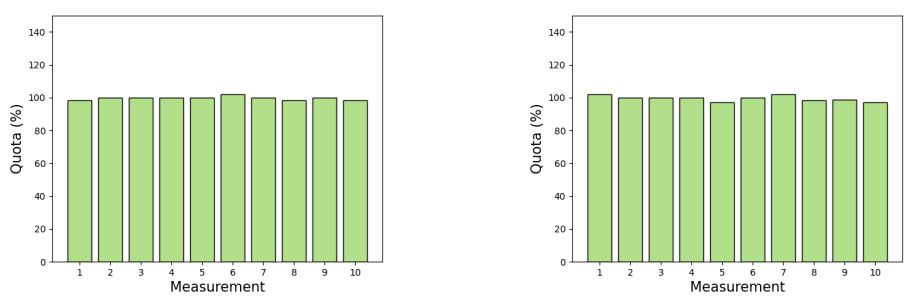

(a) The results for person 1. **(b)** The results for person 2.

Figure 4.13: Quotas between the number of minima in the sensor signal and the number of R peaks in the ECG signal when using the new measurement method.

Each measurement was one minute long and was done with the configurations presented in table 3.3. As can be seen, all the measurements have gotten a quota of almost 100 %.

4.3 Estimation Methods

4.3.1 Minimum Detection

As mentioned, this heart rate estimation method is based on counting each minimum of the sensor signal as a heart beat. Examples of applying this method are shown in the plots in figure 4.14.

It is possible to see that the minima do not always appear at the same time as a R peak in the ECG, but in many cases it is close. In figure 4.14a it may be seen that a small minimum at approximately 42 seconds appears and therefore will be counted as a heart beat. However, there is no heart beat there according to the ECG. This is also the case for the minimum just before 50 seconds in figure 4.14b. On the contrary, there is a small minimum in figure 4.14c at approximately 31 seconds which has a corresponding R peak. Also, in figure 4.14b it is possible to see that there is a clear minimum at the end of the signal, but no corresponding R peak.

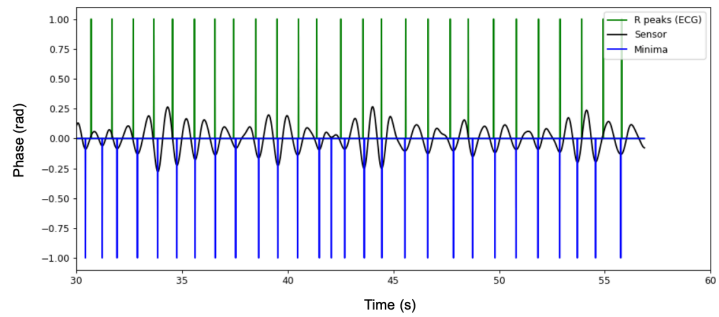

(a)

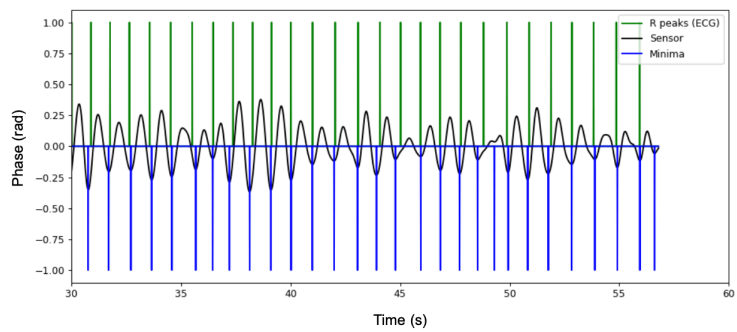

(b)

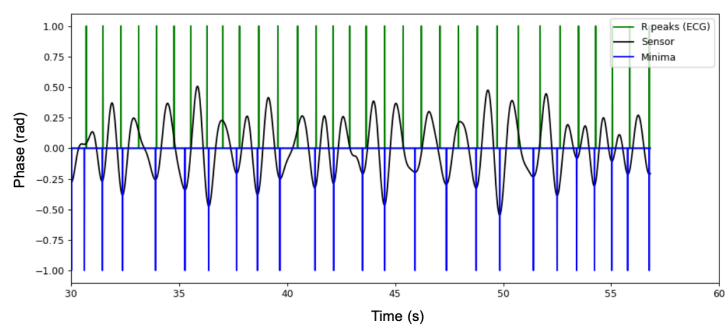

(c)

Figure 4.14: Three plots each containing a subpart of a measurement from dataset 2. The minima of the sensor signal found by the minimum detector are plotted in blue and the R peaks from the ECG signal are plotted in green.

Dataset 1

The heart rate was calculated for each sensor recording in dataset 1, in other words the measurements made at a distance of 0.7-0.9 meters with no tilting of the lens holder. The result of two of the recordings can be seen in figure 4.15 and 4.17, where the graph to the left shows the heart rate of the ECG and the sensor signal, and the graph to the right shows the FFT of the sensor signal. In figure 4.15a it can be seen that the heart rate measured by the sensor signal is similar to the ECG. According to the ECG signal, the heart rate is approximately 70 beats per minute. The sensor signal sets the heart rate to a slightly higher value than the ECG signal. By looking at the frequency plot in figure 4.15b, a peak can be found at the frequency of 1.2 Hz which corresponds to a heart rate of approximately 72 bpm.

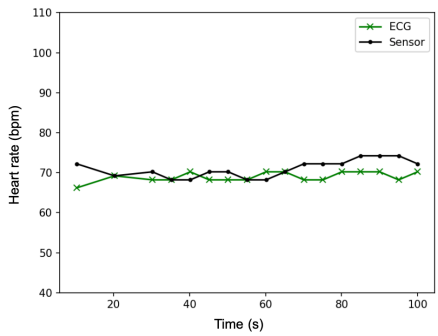

(a) The heart rates estimated by both the ECG and the sensor signal.

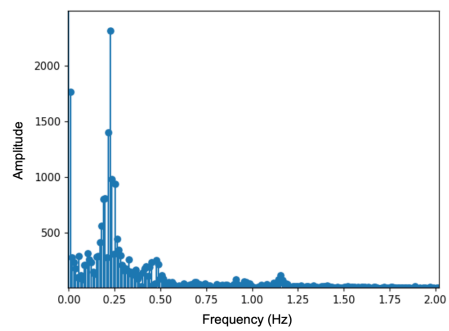

(b) The corresponding FFT of the sensor signal.

Figure 4.15: Heart rate results from dataset 1: Measurement 11.

To get a better understanding of the results given in 4.15, figure 4.16 shows the first 30 seconds of the sensor signal together with the R peaks of the ECG and minima found by this method.

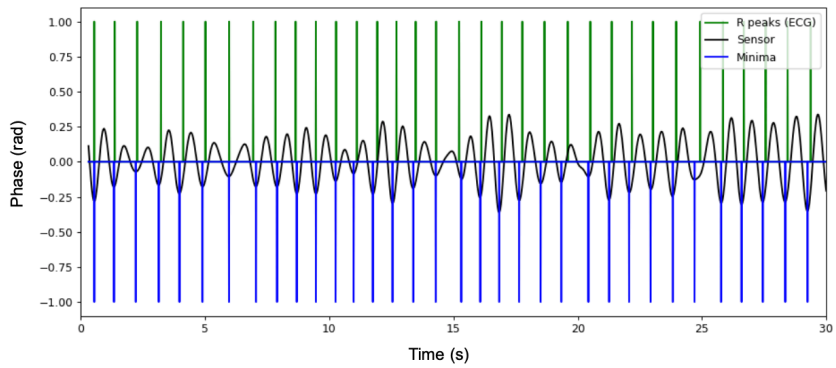

Figure 4.16: The first 30 seconds of the ECG and sensor signal presented in 4.15.

Not all recordings had as good result as the one in figure 4.15. In figure 4.17a, the measured heart rate using the sensor signal is not close to the one measured by the ECG. Also, it is not possible to visually see the heart rate from the FFT plot of the sensor signal (see figure 4.17b).

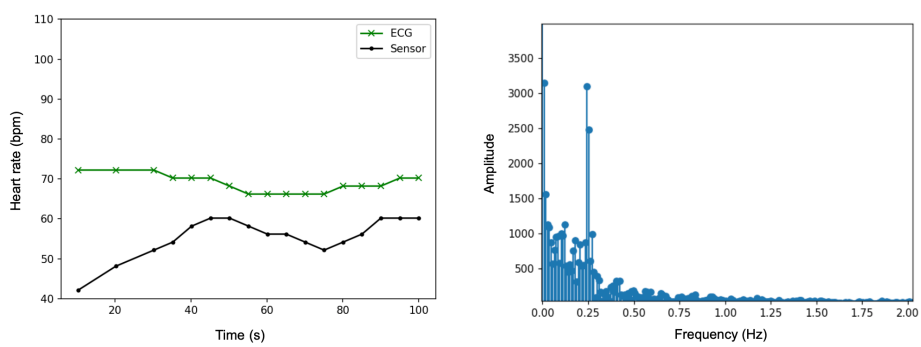

(a) The heart rates estimated by using both the ECG and the sensor signal.

(b) The corresponding FFT of the sensor signal.

Figure 4.17: Heart rate results from dataset 1: Measurement 12.

The first part of the sensor signal and the ECG signal can be seen in figure 4.18. When comparing the amount of minima of the sensor signal and the amount of heart beats in the reference ECG signal, it is clear that they are not equal nor in sync.

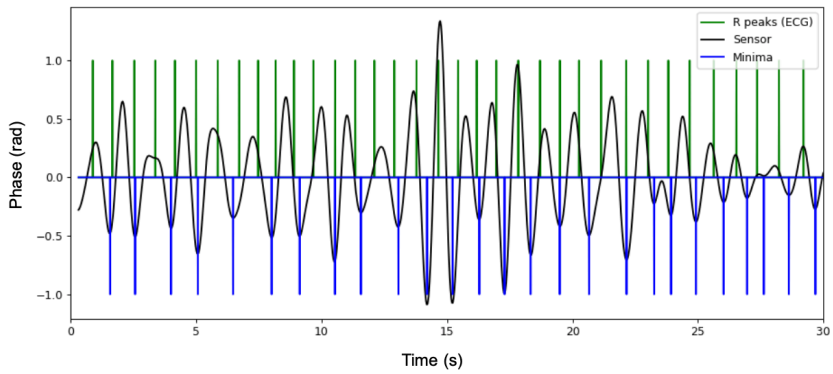

Figure 4.18: The first 30 seconds of the ECG and sensor signal presented in 4.17.

An overview of the result for all measurements of dataset 1 can be seen in figure 4.19. For each measurement the median error is presented. The reference heart rate is plotted together with the corresponding heart rate given by the sensor signal. The difference between the reference heart rate and the sensor signal is plotted as a black line to visualize the size of the error. As can be seen, most measurements have small errors.

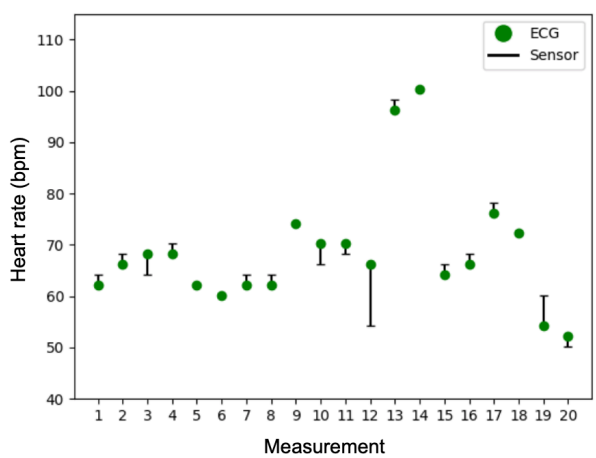

Figure 4.19: The median error between the ECG and sensor signal for each measurement. The size of the error is plotted as a vertical black line.

Dataset 2

The results for dataset 2, the measurements made with a closer distance and a tilted lens holder, is presented below.

When calculating the heart rate of the recordings in dataset 2, some results similar to the reference signal were achieved (see one example in figure 4.20). As can be seen to the left in this figure, the sensor signal gives the same heart rate estimation as the reference signal. In the FFT plot to the right, a peak can be seen at the frequency of 1.22 Hz, which corresponds to a heart rate of approximately 73 bpm. The first part of the signal is shown in figure 4.21. According to the graph, the minima of the sensor signal matches well with the actual heart beats of the ECG. This resulted in a correct heart rate.

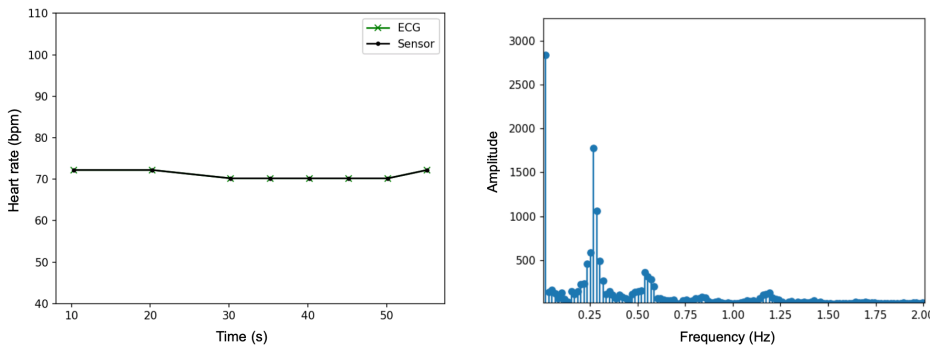

(a) The estimated heart rates. **(b)** The corresponding FFT of the sensor signal.

Figure 4.20: Heart rate results from dataset 2: Measurement 1.

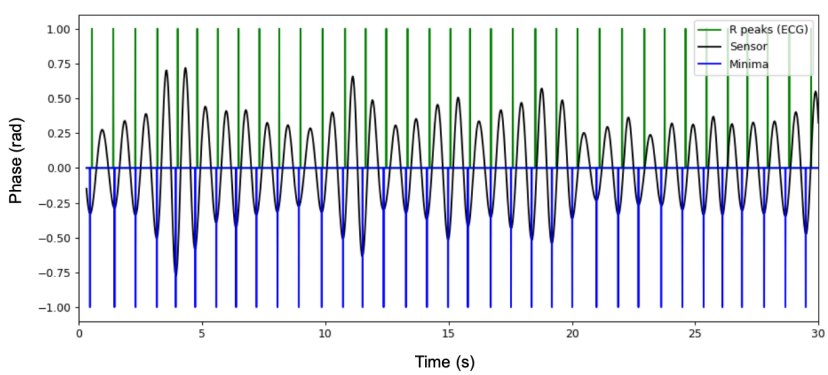

Figure 4.21: The first 30 seconds of the ECG and sensor signal presented in 4.20.

However, there were still a few recordings that did not result in a correct heart rate according to the ECG. By looking at the FFT of figure 4.22, no clear peak can be found in the range of 0.8 to 2 Hz, which is the range where the heart rate should be shown. This resulted in an incorrect heart rate, which can be seen in the graph to the left. The first part of the corresponding sensor signal and ECG signal can be seen in figure 4.23. When visually analyzing the graph, it is clear that the sensor signal does not match the ECG signal. This may be an explanation why the heart rate estimation becomes incorrect.

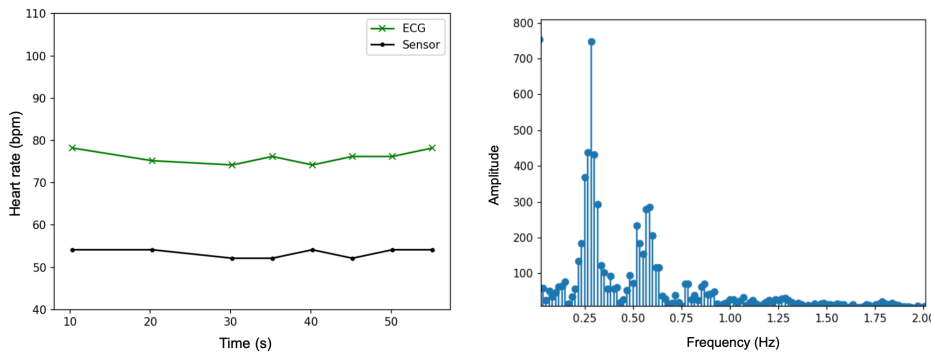

(a) The estimated heart rates. **(b)** The corresponding FFT of the sensor signal.

Figure 4.22: Heart rate results from dataset 2: Measurement 14.

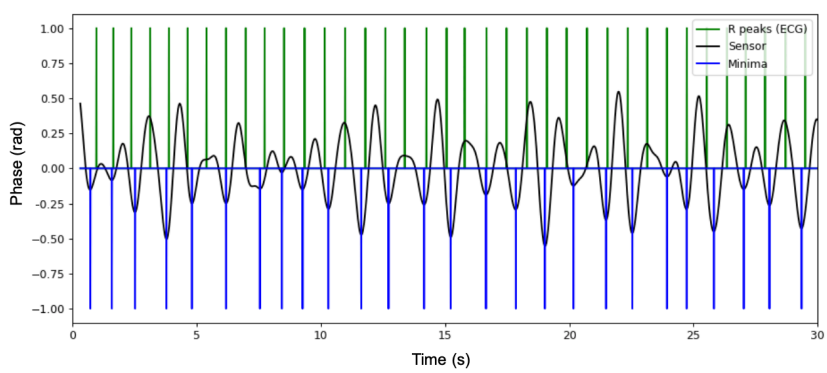

Figure 4.23: The first 30 seconds of the ECG and sensor signal presented in 4.22.

In figure 4.24 the overview of the median errors for dataset 2 are presented. For the majority of measurements, the error is quite small. Measurement 9, 14 and 20 have some bigger errors. The amount of measurements that have a median error equal to zero are more for dataset 2 than for dataset 1. However the maximum median error of dataset 2 is bigger than for dataset 1.

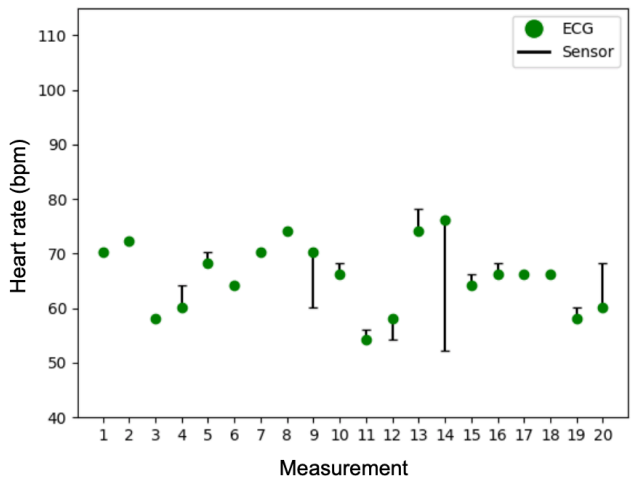

Figure 4.24: The heart rates for the median error of each measurements. The error is plotted as a vertical black line.

4.3.2 Recurrent Neural Network

The result of using the recurrent neural network to predict the heart rate is presented below. Just as before, dataset 1 and 2 are both used. The same type of test is performed to compare the heart rate between the ECG and sensor signal.

Dataset 1

In figure 4.25 the predicted heart rate of two different measurements can be seen. These are the same measurement examples as are shown in figure 4.15 and 4.17 in section 4.3.1. The measurement in figure 4.25a got a slightly worse result with this method. However, the measurement in figure 4.25b gets a better result now as the sensor curve is more similar to the ECG curve.

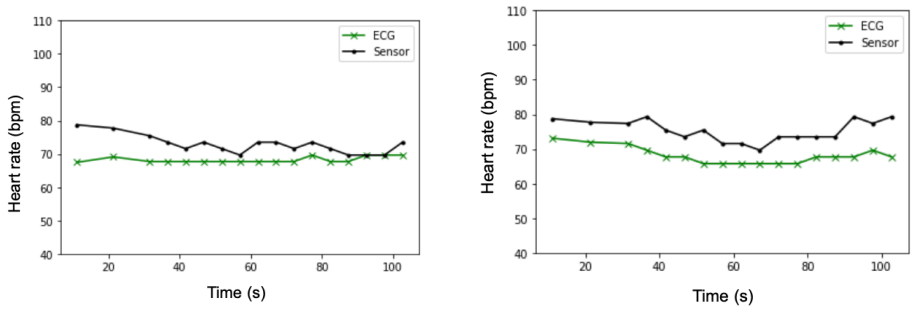

(a) Measurement 11.

(b) Measurement 12.

Figure 4.25: Heart rate plots for two measurements from dataset 1. Both the heart rate for the ECG and sensor signal are plotted.

The heart rate median error of each measurement in dataset 1 when using the recurrent neural network can be seen in figure 4.26. In general, the median heart rate error was larger when using RNN than when using the minimum detector on dataset 1.

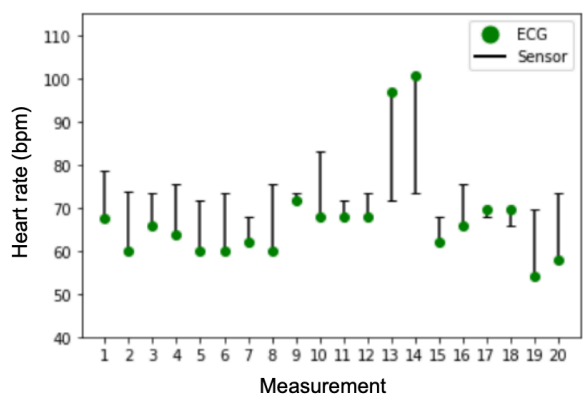

Figure 4.26: The heart rates of the median error between the ECG and sensor signal for dataset 1 when using RNN.

Dataset 2

In figure 4.27 the predicted heart rates of the same measurements presented in section 4.3.1 are plotted. The result for the measurement in figure 4.27a is good, although the result was better when using the minimum detector. On the other hand, the result for the measurement in figure 4.27b is better with this method.

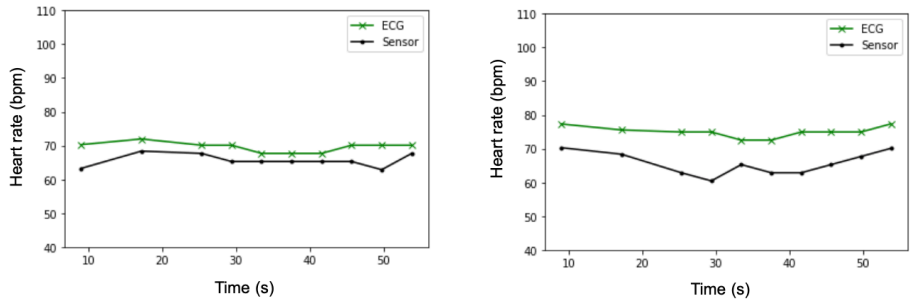

(a) Measurement 1.

(b) Measurement 14.

Figure 4.27: Heart rate plots for two measurements from dataset 2, where the result for the reference signal and sensor signal is presented.

In figure 4.28 the median heart rate error for each measurement in dataset 2 is presented. The results using the RNN for predicting the heart rate was better for dataset 2 than for dataset 1 (see figure 4.26) when visually analyzing and comparing the graphs. However, the error for most measurements were larger when using the RNN compared to the minimum detector method. There are though a few measurements, for example measurement 14, that acquires a smaller error when using the RNN method.

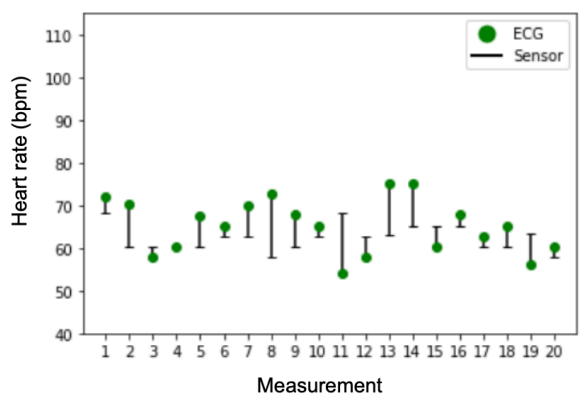

Figure 4.28: The heart rates for the median error for each measurement of dataset 2 with the RNN method.

4.4 Principal Component Analysis

The results of using PCA on one measurement from dataset 1 and one from dataset 2 is presented in this section. Both measurements belong to the same person. As

mentioned in section 2.3, the frequencies of the heart should be in the range of 0.75-3 Hz.

4.4.1 Dataset 1

Figure 4.29 shows two graphs of the Fast Fourier Transform of the unwrapped phase of a measurement in dataset 1. The graph to the right shows the FFT when only plotting the frequencies of 0.75 to 1.5 Hz, which includes the range where the frequency corresponding to the heart rate at rest may exist. As can be seen in the two plots, neither the respiration rate nor the heart rate is easy to extract.

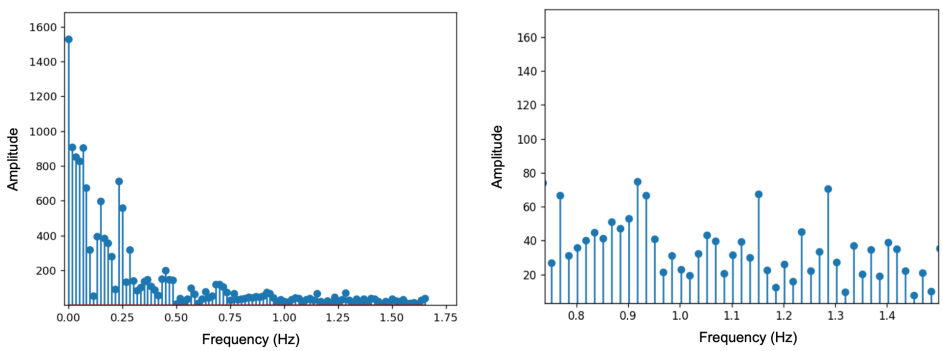

(a) FFT plot of the frequency span 0 to 1.75 Hz.

(b) Zoomed in FFT plot so that only the frequencies from 0.75 to 1.5 Hz are shown.

Figure 4.29: FFT plots of the unwrapped phase.

As mentioned in the method in section 3.5.1, the reconstruction of the signal was made using 1, 5 and 9 principal components. The FFT of each reconstruction can be seen in figure 4.30. When reconstructing with only one principal component, the majority of the frequencies gets a low amplitude. Perhaps some of the frequencies corresponding to the respiration can be seen in the plot, but the amplitudes are very small. However, when increasing the amount of principal components, more of the frequencies that probably correspond to the respiration and heart rate exist in the signal.

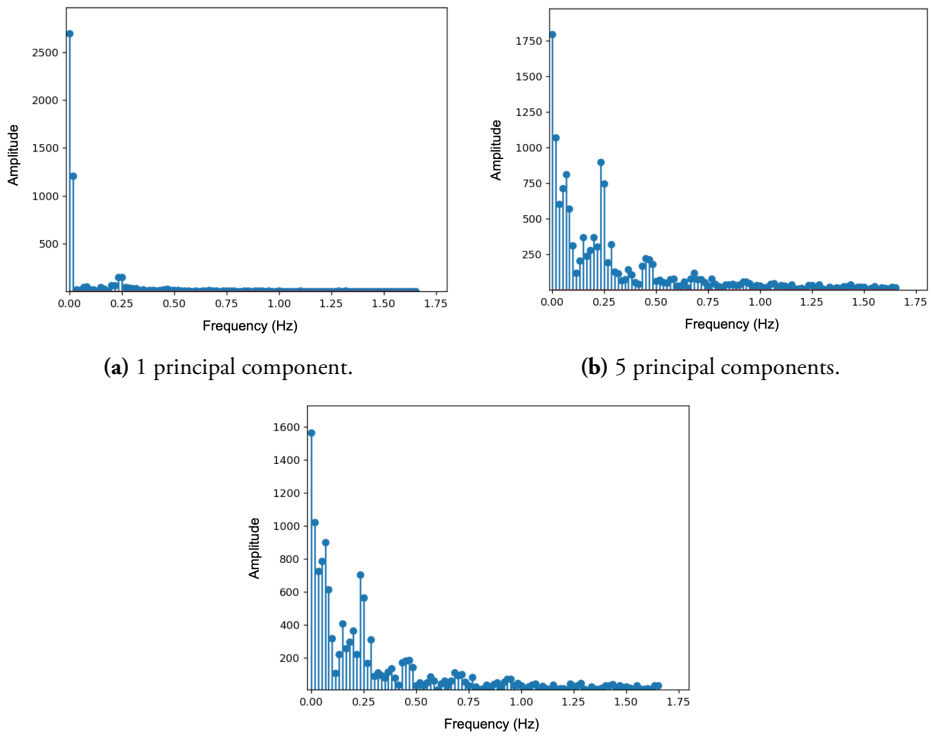

(a) 1 principal component.

(b) 5 principal components.

(c) 9 principal components.

Figure 4.30: FFT plots of reconstructing with different amount of principal components.

When removing the principal components shown in figure 4.30 from the original signal, it results in the FFT plots shown in figure 4.31. The aim of this method was to remove the respiratory activity, but still retain the heart rate. By looking at the graphs, it seems like no clear peak in the range of the heart rate can be extracted.

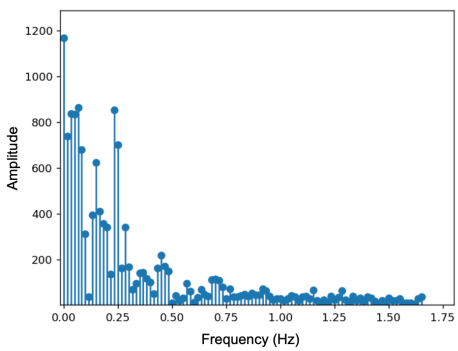

(a) Removing the first principal component.

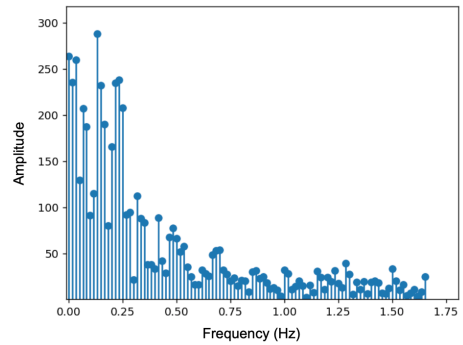

(b) Removing the 5 principal components.

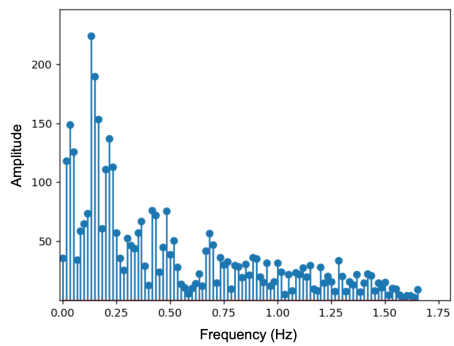

(c) Removing the 9 principal components.

Figure 4.31: FFT plots of the signal remained after removing different numbers of principal components from the original signal.

4.4.2 Dataset 2

In figure 4.32 two graphs are shown. The graph to the left shows the FFT of an unwrapped phase signal from dataset 2. To be able to visually see the possible heart rate more clearly, the graph to the right only shows the frequencies of 0.75-1.5 Hz of the signal. As can be seen in the graphs, both the respiration and the heart rate seems to be shown by just looking at the FFT plot.

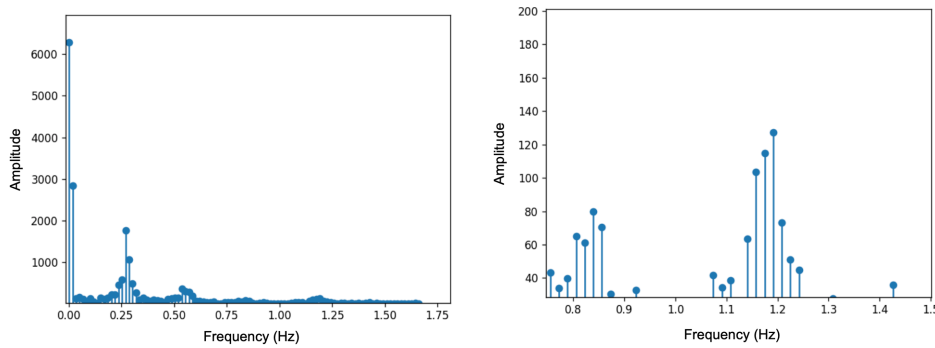

(a) FFT plot for frequencies of 0 to 1.75 Hz.

(b) Zoomed in FFT plot so that only the frequencies of 0.75 to 1.5 Hz are shown.

Figure 4.32: FFT plots of the unwrapped phase.

Just as previously, reconstructions using 1, 5 and 9 principal components were made and the results can be seen in figure 4.33. Having only one principal component seems to have removed most of the frequencies from the signal. By increasing the amount of principal components, the amplitudes of the frequencies corresponding to the respiration and the heart seems to increase.

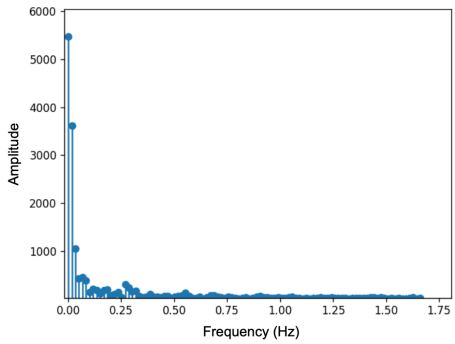

(a) 1 principal component.

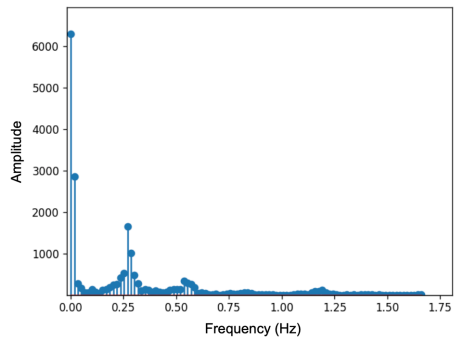

(b) 5 principal components.

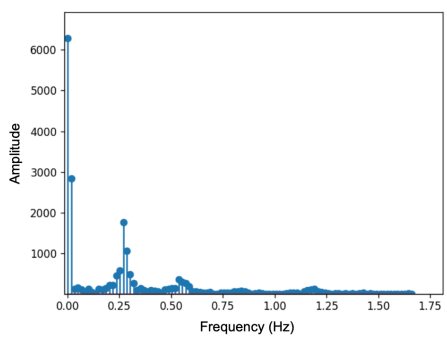

(c) 9 principal components.

Figure 4.33: FFT plots of reconstructing with different amount of principal components.

When removing the principal components shown in figure 4.33 from the original signal, it results in the FFT plots shown in figure 4.34. By removing only one component from the original signal, the majority of the frequencies corresponding to the respiration and the heart will remain. However, when increasing the amount of principal components, the amplitude of each frequency gets lower and neither the respiration nor the heart rate can be extracted easily.

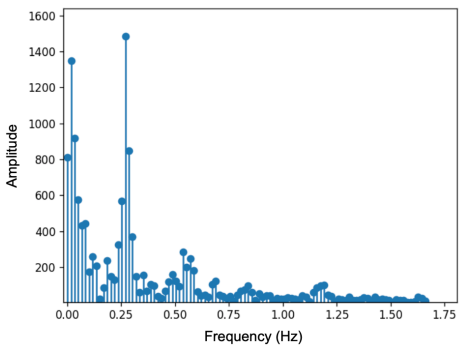

(a) Removing the first principal component.

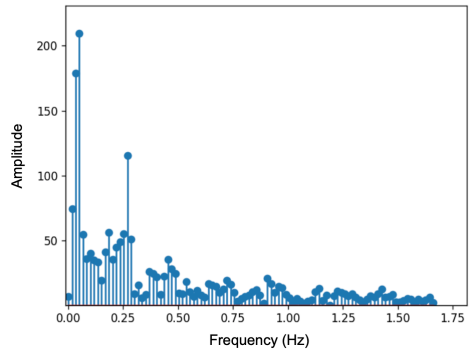

(b) Removing 5 principal components.

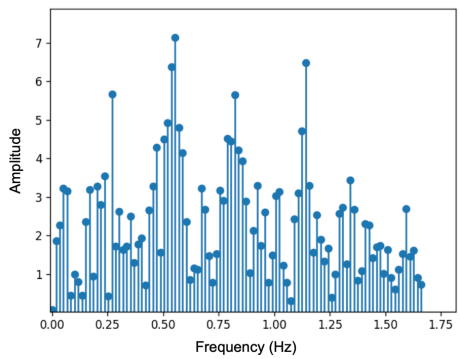

(c) Removing 9 principal components.

Figure 4.34: FFT plots of the signal remained after removing different numbers of principal components from the original signal.

Chapter 5
Discussion and Conclusion

In this section the results when using different configurations and methods are discussed. The findings of the study is analyzed and possible improvements are presented. Lastly, a conclusion is drawn and some future work is suggested.

5.1 Heart Rate Estimation Methods

As presented, the heart rates given by the sensor signal has been estimated by two different methods: The minimum detector and the RNN. When using the minimum detector, the heart rates are more similar to the reference values for both dataset 1 and 2. The neural network does not find an adequate way of detecting heart beats and is therefore outperformed by a simpler method. Possibly, the datasets are too small for the model which leads to overfitting.

As stated, this project has been scaled down to only handling heart rates at rest. Therefore, some limitations concerning acceptable heart rates have been made for both estimation methods. The minimum detector only allows two adjacent minima to appear with a time difference of at least 0.5 seconds, which induces a constraint for the highest possible heart rate. In the RNN, the window size is 40 samples, which corresponds to approximately 0.4 seconds. Therefore, if two heart beats exist within one window, it will be counted as only one heart beat. This means that heart rates up to 2.5 Hz, namely 150 bpm, can be detected using this method. The RNN-method is thus less limited regarding the maximal heart rate that can be measured. However, none of the methods can detect irregular heart beats such as extra occurring heart beats.

In summary, the minimum detector performs better than the RNN for these datasets, but has a larger limitation regarding the maximal heart rate that can be measured. However, the limitation is not an issue as the aim of this project is to measure heart rate at rest.

5.2 Evaluation Method

The evaluation method used to compare the heart rate given from the ECG and the sensor signal, see detailed explanation in section 3.4.3, is based on the R peaks and the estimated heart beats appearing at approximately the same time. However, as presented in the result, this is not always the case. A possible consequence is that some heart beats are lost at the ends of the signals, which may result in a wrong heart rate. This problem arises when the end of a segment is set between a sensor minimum and its' corresponding R peak. It will result in one more sensor minimum used to estimate the heart rate than there are R peaks. An example of this can be seen in figure 4.14b.

The majority of the evaluation points uses a time window of 30 seconds to estimate the heart rate, apart from the two first evaluation points where the time window is 10 respectively 20 seconds. A missing peak will therefore yield a larger error for the first two evaluation points. If the time window is 10 seconds, the heart rate will differ with 6 beats per minute. On the other hand, the heart rate difference will only be 2 beats per minute for a time window of 30 seconds.

Therefore, it can be said that the evaluation method can be a bit misleading when this type of situations occurs. However, it still gives an indication of how well the methods perform.

5.3 Comparison of Datasets

The datasets differed both regarding the distance to the participants and the tilting of the lens holder when performing the measurements. Yet, the result for both datasets are in general good when using the minimum detector. There are though some exceptions for both dataset 1 and 2. When analyzing the frequency plots for these measurements, no distinct peak could be distinguished in the relevant frequency span (0.8-1.9 Hz). Therefore, it seems like these measurements did not obtain the information of interest, which resulted in a wrong estimation of the heart rate.

As mentioned, two measurements were performed on each participant. Remarkably, there were no occurrences when both measurements got bad results. That is, either none of the measurements got bad results or only one of them. Therefore, it can not be said that the errors are distinctly dependent on the participant. Possibly, the errors could be caused by a change of position between the measurements.

For the measurements with clear heart rate peaks in the frequency plot, it seems like the result for dataset 2 is better than for dataset 1. As seen in figure 4.19 and 4.24 there are more measurements with the same heart rate as the ECG-signal. After further analysis it was possible to see that the minima of the sensor signals of dataset 2 had a better agreement with the R peak occurrences than the sensor signals of dataset 1, which may indicate that dataset 2 contains less noise.

Except for the change of measurement setup between the datasets, there are dif-

ferences which unintentionally may have affected the result. During the recording of dataset 1, we were not as careful when it came to removing reflective objects, for example jewelries and ECG cables, as we were when recording dataset 2. This may have caused reflections that resulted in signals containing more noise than actually necessary. Also, the measurements for each dataset were not made on the completely same persons. One theory is that the difference in the build of the body might affect the signal, and therefore the chest wall movement may differ between people. This means that it might be more or less difficult to measure depending on the person, which may have contributed to the differences in results between the datasets.

To conclude the comparison, heart rate extracting can be done successfully for almost all measurements in both datasets. However, dataset 2 seems to contain less noise when analyzing the agreement of the minima and R peaks occurrences.

5.4 Methods for Noise Removal

During the whole report, the movement caused by respiration has been a mentioned obstacle. Two different methods were tested with the purpose of removing the respiration from the signal: Bandpass filtering and Principal Component Analysis.

The boundaries of the bandpass filter are decided by the FFT of the signal. This makes the filter more adaptive to the specific signal. However, some of the measurements have quite bad FFT representation of the signal, which may result in that the wrong limits for the filter is used. Also, since we have been focusing on measuring heart rate during rest, it is not possible to use our method to measure heart rates lower than 48 bpm or higher than 114 bpm. This is a large limitation of our method and therefore it might not be the best way of deciding the boundaries of the bandpass filter.

However, when the purpose is to measure the resting pulse and the bandpass filter is applied to data with a large signal-to-noise ratio, it results in a good signal that can easily be compared to the reference signal. This sets high requirements on the recordings of the data, unfortunately it may not always be possible to meet those requirements.

The second approach to remove the respiration from the signal was to use Principal Component Analysis. In the article [11] described in section 1.2, PCA is used to extract the heart rate using the first principal component. Because of that we did not manage to reconstruct our data in a correct way when following all the steps in the article, we chose to try out another but similar method of using PCA. Our goal with using PCA was to find a better way of getting a larger signal-to-noise ratio and to separate the vital signs information into different components. Using this method it would thereafter hopefully be possible to remove the respiration from the signal to end up with a signal only containing the heart beat movements.

It can be seen in the results in section 4.4, that the frequency corresponding to the respiration movement and the frequency of the movement on the skin created by the

heart beats, existed in the same principal component. This result was similar to the articles. However, in the article the vital sign frequencies existed in the first principal component. In our case when reconstructing with only one principal component, the vital sign frequencies almost did not exist. This may depend on the differences in for example not sending in the covariance of the matrix to the data or the way of reconstructing the signal.

According to the results in section 4.4, the removal of the respiration from the original signal did not give the result we hoped for. Removing the reconstruction using one principal component from the original signal resulted in a signal still containing most of the respiration. By increasing the amount of principal components to remove from the original signal instead ended up with that almost the entire signal was removed.

The purpose of using this method was to come across with a way of avoiding the problems occurring using the bandpass filter. Unfortunately we made the conclusion that it was not possible to remove the respiration using PCA when using our data. The proposed bandpass filter was therefore the best preprocessing tool to extract the heart rate from the data.

5.5 Ethics

A vital aspect of this project has been the ethical part. This has been of the utmost importance for us when collecting the data. First of all, we informed the participants what the study would include and asked all of them for permission to collect the data. During the process, a document has been used to keep track of the name of the participant for each recording, as this could be relevant for the results. However, we decided that the presented data would be anonymous and therefore used numbers to distinguish the participants. Consequently, no sensitive information was published as the participants names were never used.

5.6 Conclusion

This work has covered different methods to measure heart rate with Acconeer's radar sensor. Mainly two things have been varied: The measurement setup and the evaluation method. The difference in result was not big regarding the measurement setup, but the best result was achieved for dataset 2, that is when having a tilted sensor with a distance of 0.4 meters to the participant. Concerning the evaluation method a larger difference in performance was shown. The evaluation method based on RNN performed worse than the minimum detector. The RNN method would possibly perform better if the datasets were larger.

This study confirmed that a major difficulty when measuring heart rate is the movement of the body caused by the respiration. The best solution we found for removing the respiration from the signal was an adaptive bandpass filter. PCA did

not work to improve the signal-to-noise ratio nor to separate the heart rate from the respiration.

In conclusion, using the minimum detector on a bandpassed filtered phase signal seems to be the best method to extract and estimate the heart rate. Dataset 2, that is the measurements recorded with a tilted lens holder on a distance of 0.4 meters, achieved the best result.

5.7 Future work

There are several parts that could be improved and further examined. The next step for us would be to investigate the reason for the variation in success level when using the minimum detector. If we could find a way of always having a strong signal-to-noise ratio for the heart rate, some further work could be done to improve the detector.

The detector is limited to only handling heart rates at rest. In order to explore the possibility of detecting higher heart rates, we would like to test to widen the range of relevant frequencies, especially to include higher frequencies. Another downside of the minimum detector is that it can not handle drastic changes in heart rate, due to that the data is filtered with a narrow pass band. This has not been a problem in this work as the recorded measurements are maximum two minutes long. If the measurements are recorded during a longer time, one solution is to update the filter boundaries after a certain amount of time.

Other solutions regarding how the depth of the recorded data is chosen, can also be further investigated. It is not entirely certain that the depth with the largest variance is the one containing the movement on the skin caused by the heart beats. It would therefore be good to examine other solutions, for example look at all the depths instead of only one.

References

[1] Abdi H., Williams L.J. (2010), *Principal component analysis*, https://wires.onlinelibrary.wiley.com/doi/pdf/10.1002/wics.101?casa_token=kVW0RUnLY4AAAAAA%3AE_JKIcIJU8ZS2GXQcc8Z5SwJQ397Wed9iAsyWyU8qXr1wh8G4HX62dXKBUOrEklNxdZ5jlePYupOb0g (Accessed: 18 March 2022).

[2] Acconeer (n.d.), *Customer stories*. Available at: https://www.acconeer.com/customer-stories/ (Accessed: 18 March 2022).

[3] Acconeer (2022), *Acconeer Exploration Tool*, Github. Available at: https://github.com/acconeer/acconeer-python-exploration (Accessed: 26 January 2022).

[4] Acconeer (2020), *Getting Started Guide*. Available at: https://developer.acconeer.com/download/getting-started-guide-lenses-pdf (Accessed: 11 March 2022).

[5] Acconeer (2021), *Radar sensor introduction*. Available at: https://docs.acconeer.com/en/latest/sensor_introduction.html (Accessed: 10 Febuary 2022)

[6] Blackledge M. J. (2006), *Digital Signal Processing*, p.134 , Elsevier.

[7] Blair D.P. and Spathis A.T. (1980), *SOME ASPECTS OF DIGITAL FILTERING TECHNICAL REPORT No. 118*. Available at: https://publications.csiro.au/rpr/download?pid=procite:cd6d958e-2774-47bc-b4f1-5532e7f77e3b&dsid=DS1 (Accessed: 24 May 2022).

[8] Brigham E.O., Morrow R.E. (1967), *The fast Fourier transform*, Available at: https://ieeexplore.ieee.org/stamp/stamp.jsp?arnumber=5217220&casa_token=RqeMr0oUbXMAAAAA:ykvHAxZiWoNl0ujhyqDV_Xi_t-K59tx_0iWngrTYm0dNRRQlYTatgwlsxgfUo0M3DlZzx9i4lw(Accessed: 18 March 2022).

[9] Gdeisat M., Lilley F., *One-Dimensional Phase Unwrapping Problem*, Available at:https://www.ljmu.ac.uk/~/media/files/ljmu/about-us/faculties-and-schools/fet/geri/onedimensionalphaseunwrapping_finalpdf.pdf(Accessed: 22 March 2022)

[10] Graves A. (2012), *Supervised Sequence Labelling with Recurrent Neural Networks*, p.14, 31-35, Toronto, Canada: Springer.

[11] Khanh L.D., Duong P.X. (2020), *Principal Component Analysis for Heart Rate Measurement using UWB Radar*, Available at: https://www.researchgate.net/publication/346125173_Principal_Component_Analysis_for_Heart_Rate_Measurement_using_UWB_Radar/fulltext/5fbc6a1392851c933f519c34/Principal-Component-Analysis-for-Heart-Rate-Measurement-using-UWB-Radar.pdf?origin=publication_detail(Accessed: 18 March 2022).

[12] Lin Z., Wang B., Chen H., Zhang Y., Wang X-A.(2017), *DESIGN AND IMPLEMENTATION OF A HIGH QUALITY R-PEAK DETECTION ALGORITHM*, IEEE [online]. Available at: https://ieeexplore.ieee.org/abstract/document/7919897?casa_token=Z1LUVdCBcBQAAAAA:n7CJiV1gG2PzjPl1UU5XnuFV2LnWrR1uGQ4WnjneU-mlyJu-dMNnLOdr72xS8pucu9_HOpUeBdU (Accessed: 10 February 2022).

[13] Ling W-K. (2007), *Nonlinear Digital Filters - Analysis and Applications*, p.8-31, Elsevier.

[14] Lumen Learning (n.d.), *Cardiac Muscle and Electrical Activity*. Available at: https://courses.lumenlearning.com/suny-ap2/chapter/cardiac-muscle-and-electrical-activity/ (Accessed: 11 March 2022).

[15] Lyons G. R., (2011), *Understanding Digital Signal Processing*. 3rd edn, p.8, 441-442, 869-870, 895, 898-899. Michigan: Pearson.

[16] Malesević N., Pertović V., Belić M., Antfolk C., Mihajlović V., Janković M. (2020), *Contactless Real-Time Heartbeat Detection via 24 GHz Continuous-Wave Doppler Radar Using Artificial Neural Networks*. Available at: https://www.mdpi.com/1424-8220/20/8/2351/pdf (Accessed: 25 January 2022).

[17] Månsson, E. (n.d.). *A121 user guide draft*. Unpublished.

[18] Nationalencyklopedin (n.d.), *Ekg*. Available at: https://www-ne-se.ludwig.lub.lu.se/uppslagsverk/encyklopedi/l%C3%A5ng/ekg (Accessed: 3 March 2022).

[19] Nationalencyklopedin (n.d.), *hjärta*. Available at: https://www-ne-se.ludwig.lub.lu.se/uppslagsverk/encyklopedi/l%C3%A5ng/hj%C3%A4rta (Accessed: 3 March 2022).

[20] Nationalencyklopedin (n.d.), *filter*. Available at: https://www-ne-se.ludwig.lub.lu.se/uppslagsverk/encyklopedi/l%C3%A5ng/filter (Accessed: 9 May 2022).

[21] Nationalencyklopedin (n.d.), *frekvens*. Available at: https://www-ne-se.ludwig.lub.lu.se/uppslagsverk/encyklopedi/l%C3%A5ng/frekvens (Accessed: 18 May 2022).

[22] Python (n.d.), *math — Mathematical functions*, Available at: https://docs.python.org/3/library/math.html (Accessed: 30 May 2022).

[23] Richards M. (2014), *Fundamentals of Radar Signal Processing*. 2nd edn, p.2-18. New York City: Mc Graw Hill Education.

[24] Richards M., Scheer J., Holm W. (2010), *Principles of Modern Radar*, Vol. I: Basic Principles, p. 3-7, 19-20, 23, Edison (NJ) : SciTech Publishing.

[25] Shafiq, G., Veluvolu, K. C. (2014), *Surface chest motion decomposition for cardiovascular monitoring*. Scientific reports, vol. 4, 5093. Available at: https://doi.org/10.1038/srep05093 (Accessed: 4 March 2022).

[26] Sharma S., Sharma S., Athaiya A. (2020), *ACTIVATION FUNCTIONS IN NEURAL NETWORKS*, Available at: https://www.ijeast.com/papers/310-316,Tesma412,IJEAST.pdf(Accessed: 23 March 2022).

[27] Smith S.,(1998), *The Scientist and Engineer's Guide to Digital Signal Processing*, p.225-226, 328 and 330-331, California Technical Pub.

[28] Sörnmo L., Laguna P. (2005), *Bioelectrical Signal Processing in Cardiac and Neurological Applications*, p.411-413, 457, 469, 487-489, Elsevier Inc.

[29] TensorFlow (2022), *Recurrent Neural Networks (RNN) with Keras*. Available at: https://www.tensorflow.org/guide/keras/rnn (Accessed: 10 February 2022).

[30] Texas Instruments (2020), *The fundamentals of millimeter wave radar sensors*. Available at: https://www.ti.com/lit/wp/spyy005a/spyy005a.pdf?ts=1647870208467&ref_url=https%253A%252F%252Fwww.google.com%252F (Accessed: 21 March 2022).

Postface

The authors' of this master thesis have participated equally and have collaborated in each part of the report. The reason for this was to be able to learn as much as possible and to contribute with different knowledge to the work. In conclusion, this working method has become successful.